EVALUATION OF THE POTENTIAL OF KERICHO AQUIFER AS A SOURCE OF GROUNDWATER

ABIGAIL CHEPKEMOI

MASTER OF SCIENCE

(Soil and Water Engineering)

JOMO KENYATTA UNIVERSITY

OF

AGRICULTURE AND TECHNOLOGY

2024

Evaluation of the Potential of Kericho Aquifer as a Source of Groundwater

Abigail Chepkemoi

A Thesis Submitted in Partial Fulfilment of the Requirements for the Degree of Master of Science in Soil and Water Engineering of the Jomo Kenyatta University of Agriculture and Technology

2024

DECLARATION

This thesis is my original work and has not been presented for a degree in any other University

Signature……..Date.....

Abigail Chepkemoi

This thesis has been submitted for examination with our approval as the University Supervisors

Signature……..Date.....

Prof. Patrick G. Home, PhD

JKUAT, Kenya

Signature……..Date.....

Prof. (Eng). James M. Raude, PhD

JKUAT, Kenya

DEDICATION

I dedicate this work to my children, mum, brothers and sisters, and the people of Kericho.

ACKNOWLEDGEMENT

Foremost, I would like to express my sincere gratitude to my advisors Prof. Patrick G. Home and Prof. (Eng). James M. Raude, the Department of Soil, Water and Environmental Engineering in the School of Biosystems and Environmental Engineering, Eng. Dr. Clement Kiprotich Kiptum, Dean of the School of Engineering, University of Eldoret and classmates for their continuous support and guidance in the development of this thesis.

I must express my very profound gratitude to my mum and my children (Ryan Kipkorir, Ray Kiptoo and Reagan Kiplangat) for providing me with unfailing support and continuous encouragement throughout my year of study and through the process of researching and writing this thesis. This accomplishment would not have been possible without them.

TABLE OF CONTENTS

LIST OF TABLES

LIST OF FIGURES

LIST OF PLATES

LIST OF APPENDICES

ACRONYMS AND ABBREVIATIONS

CC	Correlation Coefficient
CVFD	Control-Volume Finite-Difference
DO	Dissolved Oxygen
ESE	Estimated Standard Error
GIS	Geographical Information System
GMS	Groundwater Modeling System
IWM	Integrated Water Management
JMP	Joint Monitoring Program
KNP	Kenya National Policy
MODFLOW	Modular Groundwater Flow Model
MWD	Ministry of Water and Development
RMSE	Root Mean Squared Error
SEE	Standard Error of the Estimate
WRSD	Water Resources System Dynamics
WWB	World Water Balance

ABSTRACT

Groundwater is a major source of water supply in Kericho County, Kenya. However, this water source is threatened by the rise in the human population and climate change. Under these conditions, it is crucial to assess the sustainability of the groundwater resource in Kericho County. Thus, this study aimed to characterize hydraulic and hydrogeological parameters controlling groundwater occurrence and also to investigate the potential of groundwater in Kericho County, Kenya. To achieve this objective, the study utilized a combination of geophysical and pumping test data. Consequently, fifty Vertical Electric Soundings (VES) were carried out to determine the aquifer properties of the study area. Further, seven out of fifty surveyed sites were drilled to depths ranging between 30m and 230m, and test pumping was done for 24 hours. The GIS-based conceptual groundwater model was developed using Groundwater Modelling System (GMS) software. The model was calibrated in a steady state. Geophysical results show that the average hydraulic conductivity in the study area varies from 1.96 m/day to 6.2 m/day. The transmissivity ranged from 35.83 m^2/day to 5166.4 m^2 /day, while the yield ranged between 0.7 and 9.7 m^3/hr. The aquifer hydraulic parameters determined from geophysical and pumping test data were analysed using one-way analysis of variance (ANOVA). The results show no significant difference ($p = 0.95 > 0.05$) on hydraulic conductivity between geophysical and pumping test methods. Results from calibration showed hydraulic conductivity values varying from 0.28 to 1.12 m/d, while the recharge rates ranged from 0.5 to 2.2 x 10^{-4} m/d. A predictive run was done in the calibrated model to examine the aquifer's response to abstractions under three different scenarios of increasing water demand due to population growth; the effects of climate change and a combination of both increasing water demand and climate change. The results showed that excessive pumping rates interfere with the surface water and groundwater interactions. Also, locations near the river recorded a slight decline in the constant head. However, the recharge rate was higher than the abstraction, indicating that groundwater will remain sustainable as the primary source of water supply for the residents. Moreover, the volumetric budget for the three scenarios shows that the aquifer has sufficient water supply to be used by the population despite the effects of climate change and population growth. These findings provide vital information for the sustainable and effective planning and management of groundwater resources for the Kericho Aquifer

CHAPTER ONE

INTRODUCTION

1.1 Background Information

Groundwater is a natural resource stored in underground reservoirs (rocks) and transmitted through interconnected spaces (Matos, Carneiro & Silva, 2019). Groundwater is any water that lies in aquifers beneath the land surface. Its characterization distinguishes the ground depth of water, current flow, conductivity, salinity, pH, Turbidity, Dissolved Oxygen (DO), nitrate, and water temperature. Furthermore, groundwater is one of the sources of fresh water, and its importance for every form of life in the ecosystem is inevitable (Holland et al., 2015). Thus, the need to utilize groundwater sustainably.

Globally, groundwater is an essential source of water supply. However, only about 3% of the earth's total water is fresh. Groundwater comprises 95%, surface water 3.5%, and soil moisture 1.5%. Moreover, of the total fresh water on earth, only 0.36% is readily available (Pervez & Henebry, 2015). These approximations compel government institutions to take strict initiatives to conserve water resources. This will ensure adequate water supply to the current and future generations. However, climate change, urbanization, economic development, rapid population growth, and intensive industrialization have rendered groundwater vulnerable to contaminants in the past three decades. Once the groundwater is susceptible, its quality starts deteriorating, risking environmental sustainability and preservation of life. The key risks to freshwater resources are over-exploitation, over-consumption and climate change. The aforementioned factors have resulted to water scarcity being prevalent around the globe, and groundwater exploitation emerges as an alternative to meet the increased water demands **(**Shaban et al., 2006).

Groundwater is one of the nation's most critical natural resources in the United States. It provides about 40 percent of the nation's public water supply. More than 40 million people, including most of the rural population, obtain their drinking water from domestic wells (Ferrer et al., 2019). Groundwater is also the source of much of the water used for irrigation. It is the nation's principal reserve of fresh water and represents much of the potential future water supply (Perrone & Jasechko, 2017).

Regionally, in Sub-Saharan Africa, groundwater reserves are estimated to be 20 times larger than the water stored in lakes and reservoirs. These freshwater stores flow in rocks and sediment beneath the earth's surface. They are a vital source of drinking water in Sub-Saharan Africa and often the only freshwater supply in rural areas year-round. However, the demand for groundwater has also increased in towns and cities recently.

In South Africa, groundwater occurrence is characterized by the large variety of geological structures and the climatic differences that condition the regional hydrogeological settings. Crystalline rocks cover approximately 60 to 65% of the region, with aquifer systems developed in the weathered regolith and the fractured bedrock. The aquifers are largely unconfined, locally developed, and not spatially extensive. Groundwater is the largest water supply source for domestic water supplies in the Southern African Development Community (SADC) region. At the same time, it also plays a significant role in stock watering and other uses. Its contribution to total utilization in the area is estimated at 11.6% by volume, while domestic supplies contribute approximately 20% by volume (Ferrer et al., 2019).

Kenya’s population relies on surface water resources from rivers, lakes, and dammed reservoirs in addition to groundwater. Dependence on groundwater is highest in rural areas and the coastal zone. The reliance on groundwater is also increasing in some urban areas. Unfortunately, access to improved water supplies in rural areas remains low, and in urban areas, water supply declined from 92% in 1990 to 82% in 2015 (JMP, 2015).

Kenya's total potential groundwater resource (storage) is estimated to be 619 million m^3. The total groundwater abstraction rate in 2012 was estimated at 7.21 million m^3/year, and the total safe abstraction rate in Kenya is estimated to be 193 million m^3/year (JICA, 2013). Groundwater exploitation has considerable potential to boost water supplies in Kenya. However, its use is limited by poor water quality, overexploitation, climate change, saline intrusion along the coastal areas, and inadequate knowledge of the resource occurrence (Chalala et al., 2017). Despite the diminishing quality and quantity of surface water (Adeola, 2019) in Kenya, minimal studies have been conducted to assess the potential of groundwater for future water supplies. Thus, this study aimed to evaluate the potential of Kericho aquifer as a sustainable groundwater source. Kericho Aquifer is part of the larger aquifer called Kabatini aquifer that occurs within the volcanic rocks of the Nakuru area.

1.2 Statement of the Problem

Groundwater sustainability in Kericho is at risk due to over-exploitation occasioned by the increasing population, which needs groundwater to supplement surface water. Kericho County government plans to drill additional boreholes to meet the increasing demand for water in the region. However, no records are available showing that studies have been conducted to assess the potential of groundwater resources in the county (Kericho Cidp 2018-2022). Prolonged groundwater withdrawal from an aquifer in quantities exceeding average annual replenishment would result in groundwater depletion, thus, necessitating the need for this study.

Kenya's policy framework (Water Act, 2016) recognizes groundwater as a critical land-based resource. However, the treatment of groundwater in policy statements is cursory. Groundwater is dealt with under the general umbrella of water resources, and its significance is muted. No specific policy statements are made to facilitate groundwater resources' sustainable use and management (Mwiathi et al., 2022). Therefore, this study was prompted to fill the gap by evaluating the potential of Kericho aquifer as a

sustainable source of water supply and thereby inform decision-making on good groundwater management.

1.3 Objectives

1.3.1 Main Objective

The main objective of this study was to evaluate the potential of Kericho aquifer as a groundwater source.

1.3.2 Specific Objectives

The specific objectives of this study were to:

i. Evaluate the characteristics of Kericho Aquifer in terms of yield, hydrogeological and hydraulic parameters.
ii. Determine groundwater flow of the Kericho aquifer system under the prevailing characteristics using the MODFLOW model.
iii. Assess the effect of different stress conditions on the management of groundwater for the Kericho Aquifer system.

1.4 Research Questions

i. What are the characteristics of the Kericho aquifer in terms of yield, hydrogeological and hydraulic parameters?
ii. What is the Kericho aquifer system's groundwater flow under the prevailing characteristics?
iii. What are the effects of different stress conditions on groundwater management for the Kericho aquifer?

1.5 Justification

Unregulated exploitation of groundwater in Kenya may lead to its over-exploitation. The amount of money spent on groundwater monitoring, data analysis, and groundwater development planning is minimal since most of the money is spent on groundwater exploitation. The failure by the government to manage the utilization of groundwater sustainably threatens the availability of adequate water supply in the future.

Groundwater sourced from a drilled borehole is an alternative water source for most residential homes in Kenya. If not properly managed, it may lead to groundwater depletion which may result in land subsidence. Since the advent of the devolved system of governance in Kenya, Kericho is one of the counties which has focused on drilling boreholes for the residents in each ward as an alternative source of water supply. However, information on proper planning for groundwater exploitation is not available. Integrated management of groundwater resources is therefore essential for the development of the Kericho Aquifer (Kericho CIDP, 2018-2022).

Long-term population growth and economic development place ever-increasing pressure on Kenya's fresh water supply (Knüppe, 2011). A variety of uncertainties hampers groundwater management. These include climate change, socio-economic growth, ineffective governance structures affecting resource use, regulation, protection, and implementing alternative strategies to achieve sustainable development. There is a need for the Kericho governance regime to provide the capacity to ensure effective and sustainable resource regulation and allocation.

Moreover, there is lack of data and information on the characteristics of some of the key groundwater aquifers in Kenya. The study is therefore also justified by the fact that it provides data and information that is required to characterize groundwater aquifers of Kenya.

This study provides the County Government of Kericho with management interventions to effectively manage groundwater resources, considering future demands and environmental challenges. According to Kericho CIDP (2018), it is reported that the county is yet to assess its groundwater potential. Therefore this study creates a good platform for the decision makers to fast-track the need for groundwater assessment to formulate sustainable water resource management strategies.

1.6 Scope and Limitations of the Study

This study was conducted in Kericho County, Kenya. Kericho Aquifer is part of the larger aquifer called Kabatini aquifer that occurs within the volcanic rocks of the Nakuru area. The study was however limited to the aquifer extend within Kericho County. A procedure known as single whole pumping test was employed in the study area because no observation well was available in any of the boreholes. Existing Hydrogeological surveys reports were used in this study whereas some of the boreholes have not been drilled.

CHAPTER TWO

LITERATURE REVIEW

2.1 Introduction

This chapter entails a review of previous studies relevant to the current study. It highlights various hydrological parameters, groundwater management, and ground water modelling as some of the key areas for this study. This involved review of the methods used, and results from the previous studies, and finally identification of the research gap.

2.2 Hydrogeological and Hydraulic Parameters of Aquifers

Numerous studies (Araffa et al. 2022; Ombassa et al.2022; Deep *et al.* 2021; Chepchumba, 2020; Lentswe & Molwalefhe, 2020; Moubark & Abdelkareem, 2018; Yeh, H. et al. 2015; Mallick et al., 2015) have been undertaken globally and regionally on hydrogeology and hydraulics of groundwater aquifers. The hydrogeological rock formation is essential for groundwater flow and transport conditions. The genetic type of rocks determines peculiarities of hydrogeological cross-section structure, type of porosity, values, and character of spatial heterogeneity of flow and transport parameters. Furthermore, the genetic type of geologic formations greatly determines the geochemical and mineral composition of water contained in rocks, which is of great importance to the conditions of the chemical composition of groundwater and the total dissolved solids (TDS) in the groundwater (Vsevolozhsky, 2009). Mapping of spatial distribution in hydrogeological characteristics (thickness, Transmissivity, hydraulic conductivity, and storage coefficient) in shallow and deep aquifers can be accomplished using ArcGIS, and such maps would be useful in delineating potential areas for groundwater development and simulating groundwater flow in the aquifer system (Pandey, 2011).

Pandey and Kazama (2014) evaluated the hydrogeologic characteristics of groundwater aquifers in Kathmandu Valley, Nepal. The study used experimental methodology to estimate transmissivity (T) (and then hydraulic conductivity) as a function of specific

capacity (SC). An empirical relationship between T and SC was developed for shallow and deep aquifers. The estimated T ranged from 163 to 1,056m^2/day in the shallow aquifer, and 22.5 to 737m^2/day in the deep aquifer.

Boucher et al. (2016) estimated specific yield and transmissivity using magnetic resonance in an unconfined sandstone aquifer in Niger. Information on hydrogeological characteristics was mainly acquired through field measurements such as borehole geophysical techniques and field aquifer hydraulic testing. Given these methods' cost limitations and scale applicability, low-flow recession analysis techniques that utilize streamflow data can be low-cost alternative methods. This can be realized by reverse back-calculating hydrogeological parameters based on the hydrological processes by which groundwater from aquifers is naturally discharged into rivers.

Huang and Yeh (2019) evaluated hydrogeological parameter determination in the southern catchments of Taiwan using the method of flow recession. The study adopted an experimental research methodology to determine seasonal differences in the aquifer flow regime and to estimate the following three hydrogeological parameters: hydraulic conductivity (k), specific yield (Sy), and transmissivity (T). The estimation results of the present study were compared to the field test results, which showed significant differences in the recession index "K" between the dry and wet seasons. In addition, slight differences between the estimated hydrogeological parameters and the field test results were also observed for the two sub-areas because of differences in scale. Understanding hydrogeological characteristics and groundwater flow processes in aquifers are crucial for determining sustainable groundwater resource development, as well as for hydrological management and planning.

Kuria (2013) evaluated groundwater distribution and aquifer characteristics in Kenya. The study found that aquifers within the sedimentary terrains of Northern Kenya-Kenya coast stretch over a distance of 740 km in NW-SE direction, as a continuum from Marsabit through Garissa and terminates at Lamu within the Kenyan Coast. Merti aquifer is part of this extensive aquifer system. The primary aquifer within the

sedimentary setting of Southern Kenya includes the Sabaki aquifer (at Baricho area), Tiwi Aquifer, and Msambweni. The aquifer zone is marked by saturated sandy layers within the Kilindini formation. The total storage in the northern and central parts of the sandy facies of the Kilindini formation, assuming an effective porosity of 30%, is in the order of 112 million m^3. Within the riftvalley, groundwater is confined within lacustrine sediments, weathered and fractured zones in the volcanic rocks, and sediments interbedded between volcanic rocks. Aquifers within the riftvalley include the Turkana aquifer, Baringo-Bogoria aquifer, Nakuru aquifer, and Magadi aquifer. In areas covered with basement rocks, there is no single identified aquifer with significant groundwater. Other similar studies in Kenya were conducted by Ombassa et al. (2022); Chepchumba, (2020) and Nyabari et al. (2019).

The range of variation of the specific yield, S_Y, of an unconfined aquifer is relatively small, ranging from 0.05 for fine clayey sand to 0.30 for well-rounded, perfectly sorted, very coarse sand. The specific yield is, therefore, usually estimated from the lithological data as presented in Table 2.1 (Driscol, 1986).

Table 2.1: Range of Variation of Specific Yield

Material	S_y	*Material*	S_y
Coarse gravel	23	Limestone	14
Medium gravel	24	Dune sand	38
Fine gravel	25	Loess	18
Coarse sand	27	Peat	44
Medium sand	28	Schist	26
Fine sand	23	Siltstone	12
Silt	8	Silty till	6
Clay	3	Sandy till	16
Fine-grained sandstone	21	Gravelly till	16
Medium-grained sandstone	27	Tuff	21

According to Nejad (2009), the electrical resistivity method stands out as the most commonly used technique of groundwater exploration in many arid terrains. This is because it is efficient and cheap and also gives valuable information about the aquifer

characteristics such as lithology, groundwater depth, thickness, and aquifer type, among others.

The widely used electrode configurations in VES profiling are namely; Schlumberger, Wenner, and dipole-dipole arrays. Relatively, the Schlumberger array is proven to be the most suitable for VES profiling. It is characterized by greater probing depth, better resolution, and less time-consuming field deployment compared with the other array configuration methods (Burazer et al., 2010).

2.1.1 Hydraulic Parameters

Cirpka and Valocchi (2016) stated that detailed knowledge of the distribution of hydraulic parameters in the subsurface is a prerequisite to solving problems in hydrogeology and related fields. Several investigation techniques are commonly employed to estimate the distribution of hydraulic parameters, such as hydraulic conductivity, transmissivity, and storage coefficients. From recovery test data, Peterson and Fulton (2019) determined the unconfined aquifer hydraulic properties. The inverse method was used effectively to calculate the hydraulic parameters of an unconfined aquifer using residual drawdown. Features of sensitivity coefficients of drawdown to aquifer hydraulic parameters are compared between recovery and pumping times. Drawdown data were collected during pumping and recovery periods with transducers programmed based on the log scale of time installed at each observation well. The inverse computation method calculated the four aquifer parameters using pumping test drawdown and residual drawdown. The estimated standard error (ESE) for Kz seems smaller for recovery test data, but Kr is smaller for pumping test data. The sensitivity of drawdown to each of the four unconfined aquifer parameters, Kz, Kr, S, and Sr, behaves differently during pumping or recovery. Where Kz and Kr are the vertical and Horizontal permeability respectively,S is the apparent drawdown.

Li, Xu, and Feng (2020) conducted a study on discrete fracture network (DFN) based 3D numerical approach for modeling coupled groundwater flow and solute transport in a

fractured rock mass. The hydraulic conductivity of soil, rock, or geological formation depends on various physical factors. These include porosity, particle size and distribution, arrangement of particles, and other factors. Gallardo (2016) evaluated groundwater exploration for rural water supply in an arid region of southern Argentina. The study used an experimental research design. Findings showed that hydraulic conductivity varies with particle size for unconsolidated porous media. As such, clayey materials exhibit lower values of hydraulic conductivity than sand and gravel, indicating high values of hydraulic conductivity (150 m/day for coarse gravels, 45 m/day for coarse sand, and 0.08 m/day for clay). This is so because the small particle size arrangements (fine-grained) in geological formations, though porous, are not permeable enough to allow groundwater flow within them. For instance, clay soils have small particles, hence the low infiltration rate. The typical values of Hydraulic conductivities of different geologic units and classification of transmissivity magnitude are presented in Table 2.2 (Goulburn-murray, 2015) and Table 2.3 (Krasny,1993), respectively.

Table 2.2: Typical Hydraulic Conductivity of Geological Units

Geologic unit	Hydraulic Conductivity (m/d)
Fine sand	0.02 to 17
Coarse sand	0.08 to 520
Gravel	26 to 2,592
Shale	8×10^{-9} to 2×10^{-4}
Sandstone	3×10^{-5} to 0.5
Permeable basalt	0.03 to 1,728

Source : (Goulburn-murray, 2015)

Table 2.2: Classification of Transmissivity Magnitude

Transmissivity (m^2/day)	Description	Groundwater yielding capacity
>1000	Very high	Withdrawal of great regional importance
100 – 1000	High	Withdrawal of lesser regional importance
10 – 100	Intermediate	Withdrawal of local water supply (eg.small community)
1 – 10	Low	Smaller withdrawal for local water supply (private consumption)
0.1 – 1	Very low	Withdrawal of local water supply with limited consumption
< 0.1	Impermeable	Sources for local water supply are difficult

Source: (Krasny,1993)

2.1.2 Recharge

Karamouz, Ahmadi, and Akhbari (2020) defined groundwater recharge as water moving downward through the saturated zone under the force of gravity or in a direction determined by the hydraulic condition. Natural recharge of groundwater occurs from precipitation, rivers, canals, and lakes. Recharge can be quantified from direct measurements, water balance, tracer, and empirical methods.

Recharge is often the most challenging parameter to evaluate in the hydrological cycle. Identifying recharge sources is a site-specific issue and requires an understanding of the system. Water balances and numerical models can help disregard potential sources or account for new ones. Thus, a conceptual model is needed to get preliminary values of the overall groundwater balance. There is a wide variety of methods to estimate groundwater recharge, but tools to assess the reliability of particular strategies are unavailable. Among the methods commonly used, water table fluctuation, numerical groundwater modeling, Darcy flow calculation, and the water budget method are usually applied to both point and diffuse recharge dominant groundwater basins. The reliability of these methods depends primarily on the quality of data and spatial coverage of the basin. Once the reliability level is known, water resource planners and managers assess the level of risk to aquifers, the environment, and the socio-economic development required for sustainable groundwater management. Since identifying the recharge area in a catchment is site-specific and challenging, some methods involving stable isotope

techniques and artificial tracers are often used to overcome this challenge (Yidhego, 2017).

Al Atawney et al. (2021) reviewed past studies on the impacts of climate change on groundwater recharge. The authors reported that most past studies relied on the use of process-based models to predict the impacts of climate change on groundwater recharge. Furthermore, the study reported that there are projections for decline in the quantity of groundwater globally. Accordingly, the authors recommended that researchers and decision makers need to come up with sustainable ways for the preservation of groundwater for future generation. This is in line with the current study, which seeks to determine the potential of Kericho aquifer

Pavelic et al. (2012) indicated that the main source of groundwater recharge in Kenya is precipitation. Rainwater infiltrates into the ground through the top soil, sand formations, fissured and fractured rocks or other unconsolidated rock formations and is stored in aquifers/zones at varying depths. The economical depths at which boreholes draw water for domestic supplies in Kenya are found to be about 200 to 300 m. Only a small fraction of the rainwater gets stored as groundwater in a given period. In the arid and semi-arid climatic zones, the groundwater recharge is generally in the order of 3 percent of the annual rainfall while in the humid/sub-humid zones, the recharge is about 10 percent. However, in the sandy aquifers or those in unconsolidated basaltic rocks, recharge is much higher, in the order of 30 percent of the annual rainfall.

2.2 Groundwater Management

According to Szymkiewicz (2018), sustainable groundwater management is a burning challenge in the 21st century. Manmade activities play a vital role in the depletion of the natural composition of groundwater through the disposal or dissemination of toxic chemicals and microbial matter at the land surface and into soils or through wastewater. Maxwell and Condon (2016) reported that groundwater recycling depends on aquifer depth, type, location, and connectivity. Generally, the average time of renewal of

groundwater is 1,400 years. Significantly, the renewal rate of shallow groundwater is about 15 times less than deep groundwater (Maxwell & Condon, 2016). Sustainable water supply should include efficient re-use of treated wastewater, non-excessive use of surface water, and non-depletive groundwater abstraction. Water authorities must always try to balance the needs of consumers with those of the environmental and ecological systems.

Nagraj and Chetan (2017) reported on groundwater modeling being an effective tool for managing the groundwater resource and predicting groundwater changes. A 3-D groundwater flow model, viz. Visual MODFLOW was used with two conceptual layers. The model was simulated for seven years (2008-2014) under the transient case. The results from the modeling show that for the next ten years, the water table will decrease by more than 50m in the study area. The results of the forecast scenarios suggest that increasing the groundwater heads at certain places and reducing the pumping rate will help prevent groundwater depletion.

Konikow (2013) examined groundwater depletion in the United States (1900-2008), Reston, Virginia. The study adopted an experimental research design. The authors stated that groundwater depletion is an inevitable and natural consequence of withdrawing water from an aquifer. Excessive depletion is indicated by a persistent and substantial head drop resulting from groundwater pumping at a rate higher than replenishment. The scale of the problem has been quantified globally. The Yinchuan Plain, without exception, is suffering from groundwater depletion, and the two groundwater depression cones are getting deeper and broader. A survey by the Land Resources and Monitoring Institution of Ningxia indicated that the areas of influence of the cones in Yinchuan and Dawukou had reached approximately 440 km^2 and 61 km^2, respectively, in 2012. The drawdowns of water levels at the centres of the aquifers were greater than 10 m. Although the cones have been stable in recent decades, preventing further decline in groundwater levels remains an ongoing concern.

Les et al. (2014) investigated the impacts of groundwater exploitation and climate change on wetland extension over 150 years. The study used an experimental research design.it was reported that the degree of exploitation is an important parameter and influences the impacts of groundwater pumping.

Chen et al. (2018) examined the challenges and prospects of sustainable groundwater management in an agricultural plain along the Silk Road Economic Belt, north-west China. The study found that groundwater's quality is as important as its quantity. The literature has well documented that shallow groundwater is relatively more vulnerable to contaminants underneath agricultural areas with well-drained conditions. Due to the thin and permeable unsaturated zone, the shallow aquifer (< 40 m) is at significant risk from anthropogenic activities.

Given the intensified anthropogenic activities, various chemicals, including nitrate, ammonium, and heavy metal elements (such as Cr, Ni, Pb, and Zn) can easily pass through the soil and potentially contaminate groundwater. Among the many contaminants of groundwater, nitrate is particularly common in agricultural areas due to high-N fertilizers and poor irrigation practices. Groundwater with high nitrate concentration could adversely affect human health through ingestion. In the body, nitrates can be converted to nitrites, which can interfere with the ability of red blood cells to carry oxygen. This can lead to a condition called methemoglobinemia, also known as “blue baby syndrome.” Infants under six months of age are especially vulnerable to this condition because their digestive system are not fully developed.Other chemical elements that are controlled by hydrogeological conditions also affect groundwater quality. For example, the enrichment of fluoride (F) and arsenic (As) in groundwater is primarily due to weathering of F-rich and As-rich minerals and water-rock interactions.

2.3 Groundwater Modelling

Modeling can be described as the projection of an observable and measurable physical phenomenon from the real world onto the model world, where the observables can be expressed in mathematical equations. When viewed in this sense, the origin of groundwater modeling can be traced to the pioneering works of Thiem and Theis. However, the ease with which numerical calculations can nowadays be performed using a computer resulted in the reservation of the term modeling.

Anderson, Woesner and Hunt (2015) depict that most groundwater models are developed for forecasting, but models may also reconstruct past conditions in hindcasting simulations and perform engineering calculations. There are also screening models and generic models for hypothesis testing. A model is the primary quantitative tool available in a groundwater investigation. A workflow for groundwater modeling begins with a question that addresses the modeling purpose.

According to Botha (2005), the models encountered in science (particularly physics) can be conveniently divided into one of two classes: (a) models based on simple phenomenon-dependent parameters and mathematical principles (e.g., in the theory of heat conduction in solids) and (b) models, such as the Theory of Gravitation and Quantum Mechanics where the parameters are universally valid, but require sophisticated mathematical techniques for their evaluation.

2.4 Groundwater Models

Rossetto et al. (2018) defined a model as a tool designed to represent a simplified version of reality. Therefore, a model can be a valuable predictive tool for managing groundwater resources if properly constructed. For instance, using a groundwater model, it is possible to test various management schemes and predict the effects of specific actions. Even though the validity of the predictions will depend on how well the model

approximates the field conditions. Moreover, the model can help guide data collection activities.

Park, Lee and Lee (2018) observed that several models had been used to study groundwater flow systems. They include sand tank models, analog models such as viscous fluid and electrical models, and mathematical models such as analytical and numerical models. In addition, differential equations derived from basic principles of physics can be used to derive groundwater flow, such as; an analogous system of the flow of electrical current through a resistive medium or the heat flow through a solid that operates under similar physical principles.

Park, Lee, and Lee (2018) posit that mathematical models have been in use since the 1800s and consist of a set of differential equations known to govern groundwater flow. The reliability of predictions using a groundwater model depends on how well the model approximates the field situation. Simplifying assumptions must always be made to construct a model because the field situations are too complicated to be simulated in an exact way. The restrictive assumptions needed to solve the mathematical model analytically include believing that the medium is homogeneous and isotropic. To deal with more realistic situations, it is usually necessary to solve the mathematical models using numerical techniques. When high-speed digital computers became available widely in the 1960s, numerical models became a favorable model for studying groundwater. Such models include: Multi-species Transport in 3-Dimensions (MT3DMS); Soil and Water Assessment Tool (SWAT); Constituent Transport in Two Dimensions (CT2D), and MODFLOW (Park et al., 2018).

2.4.1 Multi-Species Transport in 3-Dimensions

Multi-species Transport in 3-Dimensions (MT3DMS) is a numerical groundwater transport model developed by the United States Geological Survey (USGS) for simulating the fate and transport of multiple chemical species in three dimensions. The

model is used to study the movement of contaminants through groundwater systems and to predict their concentrations and distribution over time and space (Zhang et al., 2020).

MT3DMS uses a finite difference method to solve the three-dimensional advection-dispersion equation (ADE) for multiple species. The ADE describes the transport of a solute in a porous medium, taking into account advection, dispersion, and diffusion processes (Zong et al., 2021). MT3DMS can also account for various other processes such as sorption, decay, and radioactive decay.

The model requires input data on the hydrogeologic properties of the subsurface, such as hydraulic conductivity, porosity, and dispersivity, as well as the initial concentrations and sources of the contaminants (Zhang et al., 2020). It can be run in steady-state or transient mode, allowing for simulations of both short-term and long-term transport.

MT3DMS is widely used in environmental risk assessments, site remediation studies, and other applications where the fate and transport of contaminants in groundwater systems need to be modeled. It is often used in conjunction with other groundwater modeling software, such as MODFLOW, to simulate groundwater flow and transport simultaneously. MT3DMS can also simulate various other processes such as sorption, decay, and radioactive decay using additional equations (Ameur et al., 2021). The sorption of a solute onto a solid matrix is described using an equilibrium or non-equilibrium sorption isotherm, while the decay of a solute can be modeled using first-order or zero-order decay kinetics (Zong et al., 2021). The radioactive decay of a solute can also be simulated using the Bateman equation.

While MT3DMS is a widely-used and well-established groundwater transport model, it has some limitations. MT3DMS relies on a number of simplifying assumptions about the hydrogeological system being simulated. For example, it assumes that the porous medium is homogeneous and isotropic, that the transport processes are linear and can be represented by a single set of parameters, and that the sources and sinks of contaminants are well-defined and constant over time. In reality, hydrogeological systems can be

complex and highly variable, and the assumptions made by the model may not always hold true.

2.4.2 SWAT Model

The Soil and Water Assessment Tool (SWAT) is a widely-used hydrologic model that can be used for groundwater modeling as well as other types of water resource management applications. SWAT was developed by the United States Department of Agriculture Agricultural Research Service (USDA-ARS) and simulates the movement of water, nutrients, and sediment through a watershed (Liu et al., 2020). SWAT can be used to simulate groundwater flow by coupling the model with a groundwater flow model such as MODFLOW. The coupled model can be used to simulate the movement of water and solutes through the unsaturated zone and into the groundwater system. The model takes into account factors such as soil properties, land use, climate, and topography, which can influence the movement and fate of contaminants in the groundwater system.

The SWAT model is based on a series of equations that simulate various hydrologic processes such as infiltration, evapotranspiration, runoff, and groundwater recharge. The model also accounts for processes such as plant growth, nutrient cycling, and erosion, which can influence the quality and quantity of groundwater resources (Melaku et al., 2019). To simulate groundwater flow and transport, SWAT can be set up to use a variety of groundwater modules, including MODFLOW and the Soil Moisture Routing (SMR) module (Long et al., 2020). The model requires input data on the hydrogeological properties of the subsurface, such as hydraulic conductivity, porosity, and groundwater recharge rates, as well as data on land use, climate, and topography (Jafari et al., 2021).

However, the accuracy and reliability of the model simulations can be highly dependent on the quality and availability of input data, including data on the hydrogeological properties of the subsurface, land use, and climate. Inaccurate or incomplete input data can lead to significant errors in the model output, and can limit the usefulness of the model for decision-making.

2.4.3 Constituent Transport in Two Dimensions Model

Constituent Transport in Two Dimensions (CT2D) model is a numerical model used for simulating the transport and fate of contaminants in groundwater. The model was developed by the US Geological Survey (USGS) and is widely used for environmental impact assessment studies, groundwater management, and remediation design (Gupta et al., 2022).

The CT2D model simulates the transport of contaminants in two dimensions by solving the advection-dispersion equation, which governs the movement of solutes in groundwater (Dong et al., 2019). The model takes into account various physical and chemical processes that affect the transport and fate of contaminants, such as advection, dispersion, sorption, decay, and biodegradation. The model uses a finite difference method to discretize the two-dimensional domain into a grid of nodes and elements, and then solves the advection-dispersion equation for each node and element (Dong et al., 2019). The model requires input data on the hydraulic properties of the subsurface, such as hydraulic conductivity and porosity, as well as data on the contaminant properties, such as the initial concentration, solubility, and sorption characteristics.

In addition to the advection-dispersion equation, the CT2D model includes several other equations that simulate various physical and chemical processes, such as the mass balance equation, the sorption equation, and the biodegradation equation (Hamisi et al., 2022). These equations can be customized and calibrated based on site-specific data to improve the accuracy and reliability of the model simulations.

The CT2D model is typically used for simulating the transport and fate of contaminants in groundwater over long periods of time. It can be used to evaluate the effectiveness of different remediation strategies, such as pump and treat, in situ bioremediation, or monitored natural attenuation (Adhikary et al., 2022). The model can also be used to predict the concentration of contaminants in groundwater under different scenarios, such as changes in land use or climate (Hamisi et al., 2022). Overall, the CT2D model is a

useful tool for simulating the transport and fate of contaminants in groundwater, and can provide valuable insights into the movement and impact of contaminants in the subsurface. However, like all numerical models, it has its limitations and should be used in conjunction with other data sources and tools to ensure that the results are accurate and reliable.

The model requires simplifying assumptions about the behavior of groundwater and contaminants in the subsurface (Adhikary et al., 2022). For example, the model assumes that the subsurface is homogeneous and isotropic, and that the hydraulic and contaminant properties are constant over time. In reality, the subsurface is often heterogeneous and anisotropic, and the properties can change over time due to natural or anthropogenic factors.

2.4.4 MODFLOW Model

MODFLOW (Modular Finite-difference Ground-Water flow model) was developed by the United States Geological Survey (USGS) in the late 1970s as a tool for simulating groundwater flow in the subsurface (Chen et al., 2022). The development of MODFLOW was motivated by the need to better understand and manage groundwater resources, particularly in the context of water supply and contamination issues. The development of MODFLOW was led by a team of hydrologists and groundwater modelers at the USGS, including George F. Pinder, Mary C. Hill, and Donald L. Harned, among others (Chen et al., 2022). The initial version of the model was released in 1984, and subsequent versions have been released over the years to incorporate new features and improvements.

The primary objective of MODFLOW was to provide a flexible and powerful tool for simulating groundwater flow in a range of subsurface environments, from simple to complex (Chen et al., 2022). The model was designed to be modular, which means that it can be customized and extended with additional packages to simulate other processes that affect groundwater flow and transport, such as solute transport, subsidence and

compaction, heat transport, and unsaturated flow (Ezzeldin et al., 2018). Since its initial development, MODFLOW has become one of the most widely used and studied groundwater models in the world, with applications in a range of fields including hydrogeology, environmental engineering, and water resources management (Barbieri, 2020). It has been used to study a wide range of groundwater flow and transport scenarios, including aquifer recharge and depletion, groundwater contamination, and the impacts of climate change on groundwater resources (Barbieri, 2020).

Hariharan and Shankar (2017) reviewed Visual MODFLOW applications in Groundwater Modeling. Visual MODFLOW is a Graphical User Interface for the USGS MODFLOW. It is commercial software popular among hydrogeologists due to its user-friendly features. The software mainly uses groundwater flow and contaminant transport models under different conditions. Agriculture, airfields, constructed wetlands, climate change, drought studies, Environmental Impact Assessment (EIA), landfills, mining operations, river and flood plain monitoring, saltwater intrusion, soil profile surveys, watershed analyses, etc., are some of the areas where in recent years, the software has been reportedly used. Visual MODFLOW is a commercial Graphical User Interface for MODFLOW. The 'Waterloo Hydrogeologic company introduced it in August 1994. The main difference between MODFLOW and Visual MODFLOW is that MODFLOW uses input data in the form of text files, which makes it complex and time-consuming.

On the other hand, Visual MODFLOW uses Excel files, Surfer grids, GIS, and AutoCAD data as input files. This makes modeling user-friendly and consumes comparatively lesser execution time. Another advantage of the software is that it interprets the raw text and binary output files of MODFLOW by creating color/contour maps and charts. With this, the model results can be easily analyzed and interpreted better. Visual MODFLOW is available in two types- Classic and Flex. Both types are similar in all ways, but the only difference is that the former uses a numerical approach while the latter uses a conceptual approach.

Namitha et al. (2019) evaluated groundwater flow modeling using Visual MODFLOW. A three-dimensional finite difference modeling program, namely Visual MODFLOW, was used to study and predict the aquifer system in a drought-prone area. The base map of the study area, various layers of the geological strata and their geological properties, boundary conditions, well data, and recharge conditions were fed into the model as inputs. The model was calibrated and validated, after which future groundwater conditions were predicted. The authors found that the groundwater flow regime was significantly influenced by the boundary conditions.

Beltran (2013) used Visual MODFLOW with ArcGIS and Surfer to simulate the sub-surface water flow in and around a solid waste dumpsite in Mexico and modeled the migration path lines of contaminants. The results indicate that the flow was from SW to NE of the dumpsite, raising cocern on the possible transport of pollutants to a water extraction well for the population. Zhai (2014) assessed the drainage of a limestone aquifer. The study was carried out in a mining area. The model result identified the poor drainage condition in the eighth mining area and suggested remedial measures. Kumar (2014) developed a groundwater flow model to quantify groundwater in Choutuppal Mandal, Andhra Pradesh. The water budget estimate was also made. Wang et al. (2018) predicted the groundwater level decline downstream of a river basin under different conditions and found the period during which overexploitation of groundwater was made.

It is evident from the review that the software has found applications in a variety of groundwater flow simulation settings. This shows an optimistic research potential with the software for the future. The Middle East and Asian countries (especially China) have used the software comparatively more than other nations in modeling. The literature study shows that the same research methodologies can be adopted for similar scenarios in other countries. Some studies attempted integrating other modeling software, such as GIS, SWAP, SWAT, etc., with Visual MODFLOW. Such attempts add novelty to the research.

2.4.4.1 MODFLOW Packages

Packages can construct the Ground water flow process. There are three different types of packages used; Basic packages, Hydrological packages, and Solver packages. The hydrological packages can further be divided into the internal flow and stress packages. The different package contains, to some extent, the same subroutines, and combining some packages with the same subroutine is possible. However, not all combinations are possible. For example, two solver packages cannot be used simultaneously; the same goes for the internal flow packages. The basic package contains four procedures that are not represented in the others; these are the *Stress* (ST), *Advance in time* (AD), *Output control* (OC), and *Output* (OT) procedures. The basic package can hence be seen as mainly treating administrative tasks. The function of the internal flow package is primarily to calculate and prescribe conductance terms. The stress package can be seen as the part of the hydrological package that deals with the boundary conditions. The stress package contains the five packages primarily; *Well*, *Recharge*, *River*, *General head*, and *Drain* package, displayed in Figure 2.1. The *General head* and the *River* package treat the same feature but slightly differently.

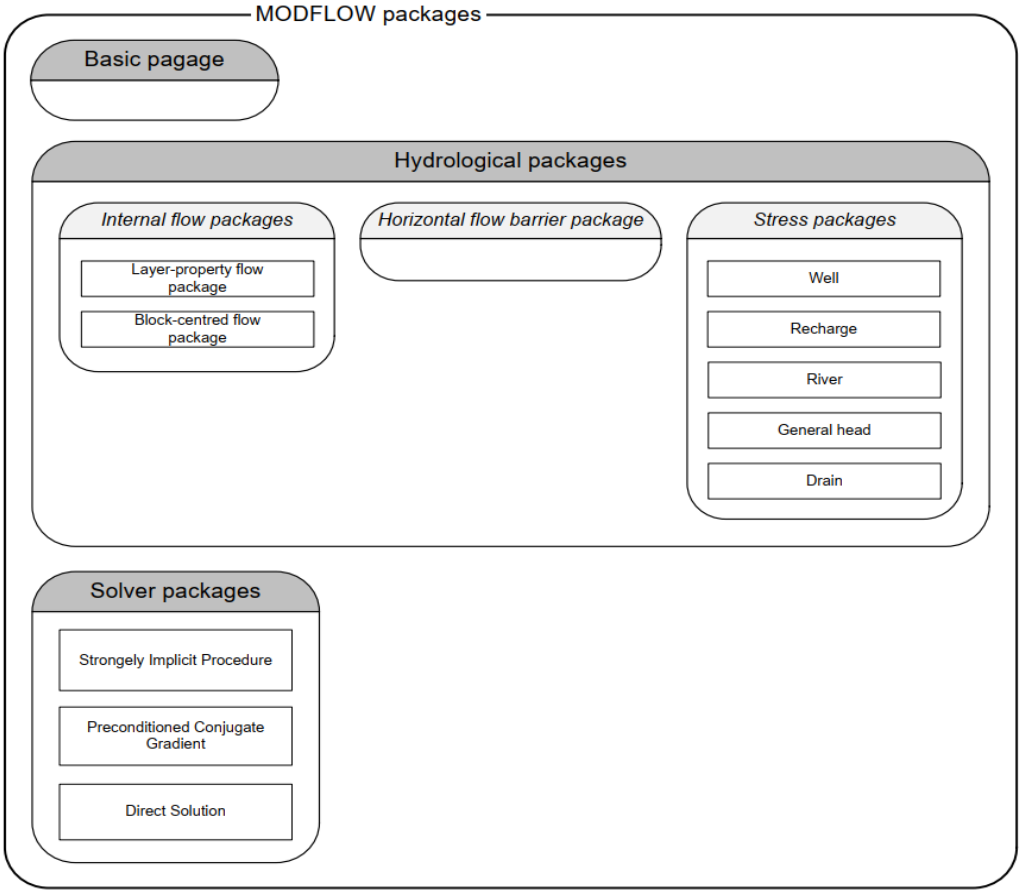

Figure 2.1: Modflow Packages

The *River* package was judged to be a more close representation of the actual behavior of a river compared to the general head package, which is why it was used here. The other packages used in the modeling were *Well*, *Recharge*, *General-head (*north and south boundary*)*, and *Drain* packages. In the solver packages, the numerical model is approximated. Three types of methods are generally possible. These are the *Strongly Implicit Procedure*, the *Preconditioned Conjugate Gradient*, and the *Direct solution*. The solver packages represent the approximate (AP) subroutine primarily. However, the FM procedure is invoked during the solution process of a nonlinear problem.

2.4.4.2 Working Principles of MODFLOW

The entire GMS consists of a graphical user interface (the GMS program) and several analysis codes (e.g., MODFLOW, MT3DMS, etc.). The first three versions of the code, MODFLOW-84, MODFLOW-88, and MODFLOW-96, were based on the initial conceptualization of the program as a groundwater-flow model only. These codes simulate specific aspects of a groundwater-flow system using independent, modular-programming components called "Packages," such as the Well Package and River Package. MODFLOW's modular design was further expanded with the release of MODFLOW-2000 by the addition of "Processes," which are parts of the code that solve a significant equation or set of related equations and that consist of sets of the underlying packages. The part of the code that solves the groundwater-flow equation became the Groundwater Flow (GWF) Process. Although other processes have been developed for MODFLOW, the GWF Process remains a core process on which other MODFLOW simulation capabilities are built. The primary change in MODFLOW-2005 from MODFLOW-2000 is the approach used by MODFLOW-2005 for managing internal data (Lee H., 2018).

MODFLOW 6 is the newest core version and uses a new format of blocks and keywords for model data input. It was written from scratch using an object-oriented design. MODFLOW 6 presently supports one type of process model, the GWF Model. Other models may be added in the future, such as a groundwater transport model, a surface-water model, and a pipe network model. Underlying MODFLOW 6 is a framework that allows developers to add new models and the interactions between models. A vital feature of the new MODFLOW 6 framework is the ability to solve multiple, tightly coupled numerical models in a single system of equations. These may be various models of the same type or different types. MODFLOW 6 is an entirely new version of MODFLOW.

2.5 Modelling Groundwater Flow

The Figure 2.2 shows the role and importance of developing the conceptual model in the entire modeling procedure.

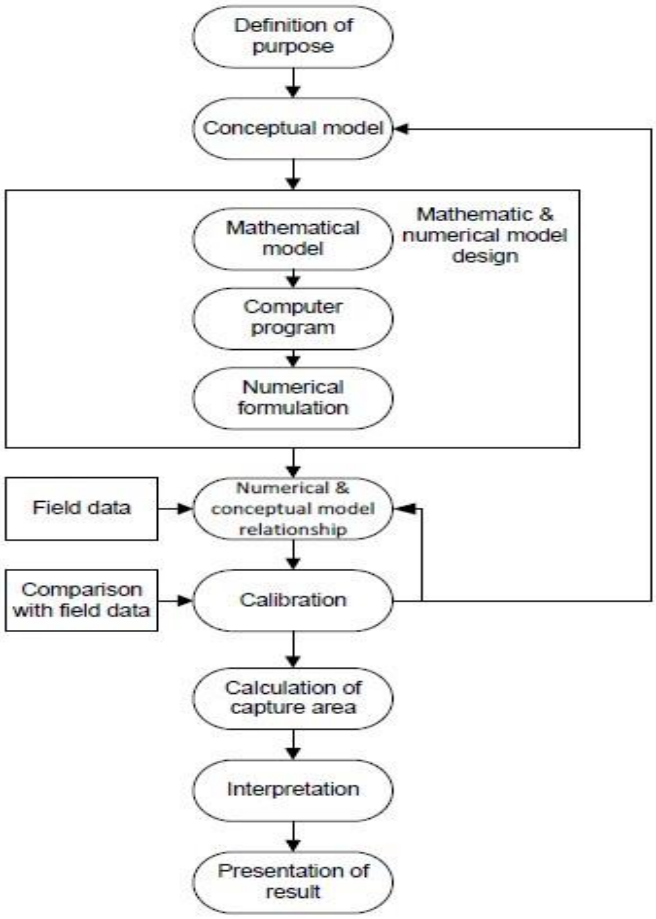

Figure 2.2: Methodology Chart Showing Steps in Developing the Entire Model

In order for a groundwater model to be accurate, reliable, and robust, it requires a large amount of data and an understanding of the aquifer. The first step in developing a groundwater model, and perhaps the most important, involves the design of a conceptual model. The conceptual hydrogeologic model forms the basis for developing the numerical model. Moreover, an increased level of effort in creating the conceptual

model reduces the effort in calibrating the numerical model (Anderson & Woessner, 1992).

The groundwater flow model was conceptualized on the basis of geological, hydro-geological and climatic characteristics of the study area. Thus, the GIS based conceptual model groundwater was developed using MODFLOW based software GMS 10.4.7 (Aquaveo, 2010). MODFLOW can solve the steady and transient groundwater flow equation and can simulate multiple or single aquifer layers with different boundary conditions (Tamma Rao et al., 2012).

Defining all grid properties and data within the model manually is tedious. The conceptual model method of building a MODFLOW model allows a user to define the model properties from GIS layers. Then, the properties of the GIS data can be transferred to the appropriate grids (Kumar, 2012).The purpose of developing a conceptual model is to formulate a better understanding of a site condition.Data collected from the boreholes are very important in groundwater modeling studies. In some cases, modeling has to be performed based on limited information because drilling records are not easily accessible to be used for modelling.

2.5.1 Governing Equation

The governing equation can be derived by combining the equation of continuity with the constitutive relation Darcy's law (Anderson & Woessner, 1992). The equation of continuity can be obtained by applying the concept of elemental Cartesian fixed control volume, displayed in Figure 2.3, and assuming that the fluid properties are considered to be uniform in time and space.

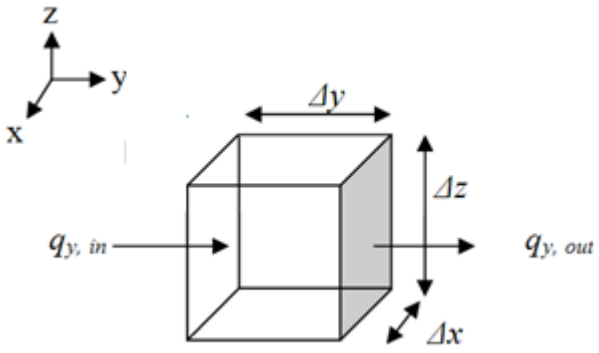

Figure 2.3: A Control Volume

ΔV=ΔxΔyΔz, representing a cube of porous material

In Figure 2.3, the flow in the y-direction, through the west and east side is shown. The area of the sides is denoted as ΔxΔz, the inflow as qy,in and the outflow qy,out. The flow through the west side can be expressed as shown in equation 2.2:

$$q_{y,in} = \nu_{in}\rho\Delta x\Delta z \tag{2.2}$$

While the flow through the eastside is as expressed in equation 2.3:

$$q_{y,out} = (\nu_{in} + \frac{\partial \nu}{\partial y}\Delta y)\rho\Delta x\Delta z \tag{2.3}$$

Where:

ϑ = Fluid velocity in the y-direction (m/sec)

ρ = Density of the fluid (assumed to be constant) (kg/m^3).

The change in flow between the east and west phases can be expressed as (equation 2.4):

$$q_{y,in} - q_{y,out} = \frac{\partial v}{\partial y}\rho \Delta y \Delta x \Delta z \tag{2.4}$$

Equations for the remaining directions could be formulated in a similar way (White, 2009). According to the conservation of mass principle, a change in inflow and outflow should be equal to the change in storage within the control-volume. The change in storage per unit change in head can be written as:

$$S_s = \frac{\Delta V\ fluid}{\Delta h \Delta V\ storage} \tag{2.5}$$

Where:

$$V_{storage} = \Delta x \Delta y \Delta z \tag{2.6}$$

A change in storage during a time, *Δt*, could be written as:

$$\frac{\Delta V}{\Delta t} = S_s \frac{\Delta h}{\Delta t} \Delta x \Delta y \Delta z \tag{2.7}$$

Accounting for the remaining directions yields:

$$\frac{\partial u}{\partial x}\rho \Delta x \Delta y \Delta z + \frac{\partial v}{\partial y}\rho \Delta x \Delta y \Delta z + \frac{\partial w}{\partial z}\rho \Delta x \Delta y \Delta z = -S_s \frac{\Delta h}{\Delta t} \Delta x \Delta y \Delta z \tag{2.8}$$

This can be simplified as shown in equation 2.9:

$$\frac{\partial u}{\partial x} + \frac{\partial v}{\partial y} + \frac{\partial w}{\partial z} = -S_s \frac{\Delta h}{\Delta t} \tag{2.9}$$

Sahoo and Jha (2017) suggest that groundwater models may be used to predict the effects of hydrological changes (like groundwater abstraction or irrigation developments) on the behavior of the aquifer and are often named groundwater simulation models.

Darcy's law in three dimensions yields is as expressed in equations 2.10 – 2.12:

$$u = -K_x \frac{\partial h}{\partial x} \tag{2.10}$$

$$v = -K_y \frac{\partial h}{\partial y} \tag{2.11}$$

$$w = -K_z \frac{\partial h}{\partial z} \tag{2.12}$$

Inserting the continuity equation and allowing for possible internal sources and sinks, yields in Equation 2.13:

$$\frac{\partial}{\partial x}\left(K_x \frac{\partial h}{\partial x}\right) + \frac{\partial}{\partial y}\left(K_y \frac{\partial h}{\partial y}\right) + \frac{\partial}{\partial z}\left(K_z \frac{\partial h}{\partial z}\right) + W = -S_s \frac{\Delta h}{\Delta t} \tag{2.13}$$

W represents internal sinks and sources within an element (Sahoo & Jha, 2017). This is the governing equation for three dimensional movement of fluid in an heterogeneous and anisotropic porous media under non-equilibrium conditions (time-dependent conditions).

2.5.2 Boundary Conditions

Correct selection of boundary conditions is a critical step in model design because the boundaries largely determine the flow pattern (Anderson & Woessner, 1992).Dirichlet

condition is a boundary condition used to define the known and fixed values of the groundwater level or hydraulic head at specific boundaries within a model's domain.Neumann condition is used in groundwater modelling to define the flux or flowrate across a specified boundary.

2.5.3 Dimensional Approach

The governing Equation is directly related to the dimensional approach. A Two-dimensional (2-D) model is appropriate if the hydraulic conductivity is uniformly approximated with depth. In a 2-D model, the flow is assumed to be strictly horizontal.

The advantage of a 3-D approach over 2-D lies in its ability to calculate the vertical head distribution within the Aquifer. Using a 3-D approach, the hydraulic conductivity in all three directions is prescribed for the whole domain rather than identifying aquifers and confining beds (Anderson & Woessner, 1992).

2.5.4 Simulation and Validation

MODFLOW numerically uses block-centered finite differences to solve the flow equations in three dimensions. It consists of a main program and independent subroutines called modules. The modules are grouped into packages, and each package deals with a specific hydrogeologic feature to be simulated (McDonald & Harbaugh, 1988).

Model validation, generally defined as a set of measurements or observations of system variables, is used for model calibration, and the remaining part is used for model validation (Anderson & Woessner, 1992).

2.5.5 Sensitivity

Scaled sensitivities are dimensionless quantities that can be used to compare the importance of different observations in estimating a simulated value (Hill, 1998).For a

selected parameter, the greater the value of composite scaled sensitivity, the greater the importance of the selected parameter.

2.6 Stress Conditions on Groundwater

Omar et al. (2020) developed A Modular Three-Dimensional Scenario-Based Numerical Modelling of Groundwater Flow, Several criteria were used during model development and calibration to determine how fine the model simulated conditions in the aquifer. Model calibration was done on the values of hydraulic conductivity and recharge rates. A rootmean square error analysis was performed during calibration to serve as a criterion to minimize differences between observed and model computed water levels. Further, calibrated model was used to analyze different scenarios to understand the future scenario of water resources. Scenario 1: Keeping in mind, the population of the study area for 2031, discharge rate (pumping rate) was increased. To compensate these demands, pumping wells were increased in the study area and model was simulated with increased discharge values. Results show that the drawdown was very uneven. At some places, it decreased more i.e. upto 6 m as compared to another prominent place where the chance of depletion of groundwater was more i.e. upto 4 m. Groundwater level was found less decreasing near the rivers due to the transfer of water from the river to the aquifer as additional groundwater discharge increases river water seepage into the adjoin aquifer. This shows that a gradual rise in the groundwater pumping can increase river seepage to the aquifer. Scenario 2: Considering the urbanization for 2031, the recharge rate was decreased to 0.00008 m/d. the lower recharge rate was taken to accommodate the decrease rainfall distribution due to climate change. Discharge rate was taken as same. Results show less change in the groundwater level as compare to Scenario-1. Scenario 3: Taking above both Scenarios simultaneously. The results show that discharge has sufficiently more domination over the recharge rate. Additional groundwater pumping can lead to change to flow direction from the aquifer to river and vice versa.

2.7 Research Gap

Despite the growing importance of groundwater management, there is a significant research gap regarding the evaluation of the Aquifer's potential as a reliable and sustainable source of groundwater. Existing studies have not comprehensively evaluated the characteristics, hydrogeological parameters, and hydraulic properties of the existing aquifers in Kericho County. Furthermore, there is a lack of understanding about the groundwater flow dynamics within the aquifer system, particularly under the prevailing hydrogeological conditions. In addition, limited research has been conducted on assessing the impact of various stress conditions on the sustainable management of groundwater resources in Kenya, and none in Kericho County. Therefore, there is a need to address these gaps through a comprehensive study that evaluates the aquifer's characteristics, employs modeling techniques such as MODFLOW to understand groundwater flow, and assesses the effects of different stress conditions on the sustainable management of groundwater resources.

2.8 Conceptual Framework

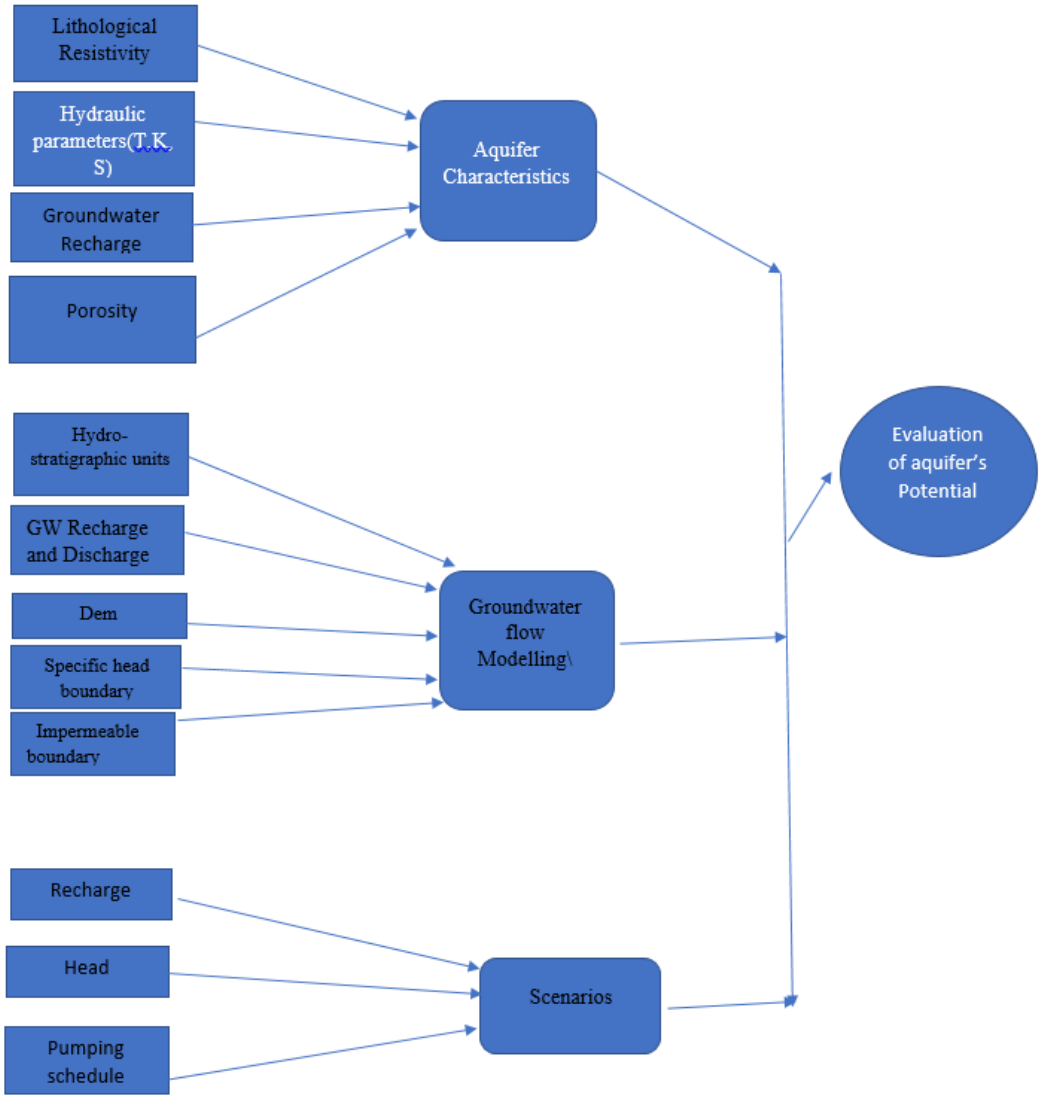

Figure 2.4: Schematic Presentation of the Conceptual Framework

CHAPTER THREE

MATERIALS AND METHODS

3.1 Study Area

The study was conducted in Kericho County located in Kenya. The study area falls within the Mau forest, which is the largest water tower in Kenya, and lies on the western part of the Rift valley. Kericho aquifer lies between longitudes 35.464540° and 35.002824° and latitudes -0.179728° and -0.505624°, with an altitude of about 2093m (Figure 3.1). The study area is mainly made up of metamorphic and igneous rocks. Intermediate igneous rocks and tertiary lavas (phonolites) dominate the county's subsurface. In addition, granites, volcanic ash mixing, and other abundant materials dominate a tiny portion of the county (Barounis & Karadima, 2011). It is largely characterised by rain forest and the mountain forest vegetation land cover types. The study is largely agricultural with cropland dominating the landscape and sub substantial urban area characterise the physical landscape of the county.

Kericho County is the leading tea growing area in the country, with the tea sector employing most of the individuals from this area. Additionally, the locals practice dairy farming and other businesses. Other crops grown in the area include maize, potatoes, pineapple, coffee, vegetables, and beans (Kericho CIDP, 2018-2022). The temperature ranges between 20-28º C, and the mean annual rainfall ranges between 1400 mm and 2000 mm (CIDP, 2018). The aquifer thickness in the area ranges between 15.1m and 404.7m.

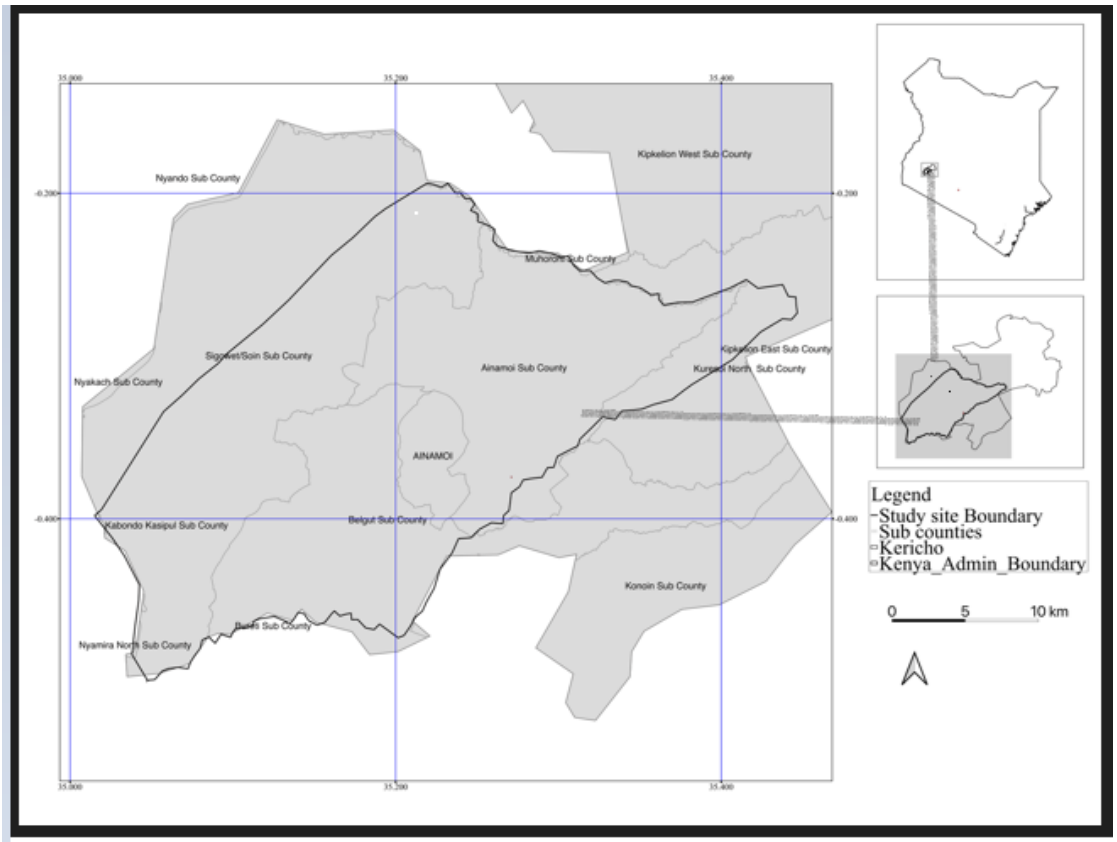

Figure 3.1: Location of the Study Site

3.2 Yield, Hydrogeological Rock Formation and Hydraulic Parameters

3.2.1 Electrical Resistivity Survey

Fifty points were located in different parts of Kericho, Kenya, using the vertical electrical sounding (VES) technique. The VES was done by employing the Schlumberger electrode configuration using an ABEM Terameter (model SAS 300B). The arrangement of the electrodes is shown in Figure 3.2 (Ashraf et al., 2018)

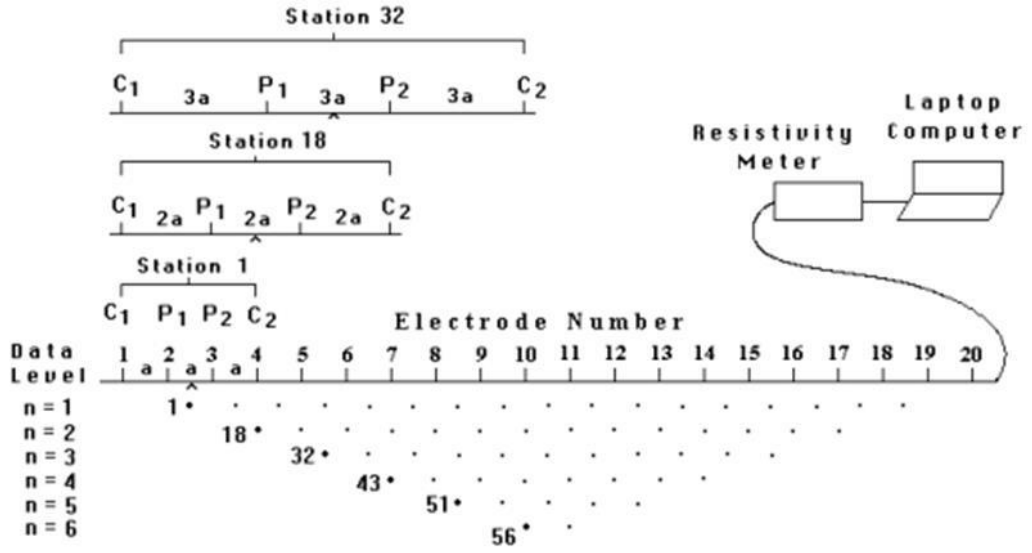

Figure 3.2: Arrangement of Electrodes for 2D Electrical Survey

The apparent resistivity values obtained were plotted on a bi-log graph against the separation spacing of the half-current electrode. After that, qualitative deductions such as the resistivity of the top layer, the curve types, and the depth of each layer were made. The first quantitative interpretations were made using the partial curve matching technique. The field curves generated were matched segment by segment with the appropriate master and auxiliary curves. Next, the thicknesses and resistivities of the various layers were improved by employing an automatic iterative computer program following the main ideas of Alva (2009). The IP2 Win computer software was used for carrying out the iteration and inversion processes.

The hydraulic conductivity was estimated using the Equation 3.1 as given by Andreia et al. (2021):

$$K = 386.40 R_{rw}^{-0.93283} \tag{3.1}$$

Where:

K = the hydraulic conductivity (m/day)

R_{rw} = the aquifer resistivity (Ω)

The transmissivity values were calculated using Equation 3.2 given as:

$$T = Kh \tag{3.2}$$

Where:

T = transmissivity (m^2/day),

H = aquifer thickness (m)

This gives an idea of the aquifer's water-producing capabilities.

The total longitudinal conductance, S_T of the overburden unit at each VES station was obtained from the mathematical relation (Zohdy et al., 1974):

$$s_T = \sum_{i=1}^{n} \frac{h_i}{\rho_i} \tag{3.3}$$

Where:

S_T = total longitudinal conductance of the overburden,

ρ = layer resistivity, Ω

h_i = layer thickness, m

n = number of layers used to characterize the aquifer protective capacity of the area.

The longitudinal conductance (S) was thus calculated by:

$$s = \frac{h}{\rho} \tag{3.4}$$

Where:

h = layer thickness of the aquifer

ρ = layer resistivity of the aquifer.

3.2.2 Pumping Test

Pumping test reports from the Kericho County Water Department and Water Resources Authority (WRA) offices were collected and used in this study. The data was divided into two categories based on their quality. High-quality data included the constant rate pumping test of at least 24 hours taken over the last four years. Pumping test data that failed to meet the above criteria were classified as poor quality (Reports from the WRA). Data used in this study were from pumping tests performed between 2017 and 2020. The pumping tests were performed as follows:

A suitable local datum such as the top of the casing was chosen from which all water-level readings and the rest-water level were measured. Then, the valve to the setting for the first step was opened, and the pumps were installed at positions determined by the specific casing design of each borehole during drilling was switched on, and the stopwatch started at the same time.

A PVC dipper tube was installed alongside the test pump rising main and tied securely to it. Each borehole was pumped at a constant rate for 24 hours, and water-level measurements were taken at regular time intervals and recorded. The water pumped from the wells was discharged at a distance to prevent flow back to the borehole under test. Twenty litres of the calibrated container were used to measure the discharge volume manually, and the time it took to fill it was recorded. The discharge rate was then calculated.

The pumping test data collected was then analyzed using Microsoft Excel 2010. The collected data during and after the pumping were analyzed to determine the following hydraulic parameters: Transmissivity, Hydraulic Conductivity, Storability and Specific capacity. Similar methods were used by other authors conducting relatively similar studies such as Zhu et al. (2020), Moharir et al. (2020) and Hasan et al. (2021).

3.2.2.1 Application of Cooper and Jacob Method

The pumping test results of the wells are plotted on semi-logarithmic paper, as presented in Figure 3.3.

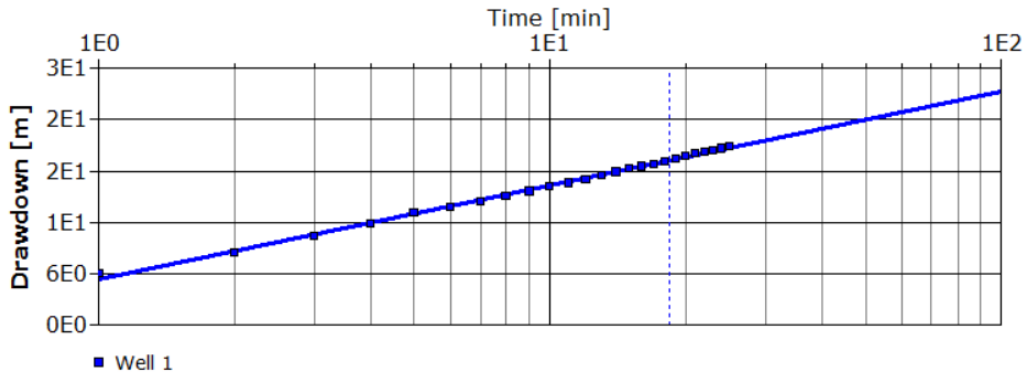

Figure 3.3: Tabsabei Borehole Time Drawdown Plot

a) Transmissivity (T)

Transmissivity T, is the rate at which water passes through a unit width of a saturated thickness of an aquifer under a unit hydraulic gradient. The Hydraulic conductivity (K) and Transmissivity (T) are related and presented as Equation 3.5:

$$T = Kb \quad (3.5)$$

Where:

T = transmissivity (m^2/day)

K = hydraulic or aquifer conductivity (m/day)

b = thickness of the aquifer (m)

The drawdown, s for a pumping well was calculated using Equation 3.6 (Cooper and Jacob,1946):

$$s = 2.3Q/4\pi T \log 2.25Tt_o/r^2 \quad (3.6)$$

Hydraulic conductivity was determined from aquifer thickness and transmissivity, while drawdown and discharge data were used to evaluate Specific capacity.

b) Specific Capacity (S_c)

Specific capacity is the discharge rate per drawdown. Mathematically, specific capacity (SC) is expressed as shown in Equation (3.7):

$$S_c = Q/S, \tag{3.7}$$

where:

Q = discharge rate (m^3/d)
S = drawdown (m)

c) Storativity (S)

According to cooper and Jacob (1946), Storativity, also referred to as storage coefficient (S), is the volume of water an aquifer releases from or takes into storage per unit surface area, per unit change in head. The non-equilibrium equation for storativity was represented using Equation (3.8).

$$S = 2.25T\frac{t_0}{r^2} \ , \tag{3.8}$$

Where:

t_o = time at zero drawdown,(s)
S = storativity of the aquifer
r = distance from the pumping well to an observation well (m)

3.2.3 Estimation of Hydraulic conductivity by VES Techinique

VES technique can be used to estimate some hydraulic properties using relationships between electrical and hydraulic properties. Hydraulic conductivity (m/s) is defined as the speed of water motion inside the porous rock. This parameter is a function of the rock and fluid (water) properties. The hydraulic conductivity for each layer can be calculated through the following relationship (Domenico ,1997):

$$k = \left(\frac{p_w g}{\mu}\right)\left(\frac{d^2}{180}\right)\left(\frac{\varphi^3}{(1-\varphi)^2}\right) \tag{3.9}$$

Where d is the particle diameter (m) and pw represents the pore fluid density (1000 kg/m3). Parameter of g indicates the gravitation acceleration, ϕ is porosity, and μ is the fluid viscosity.

Hydraulic conductivity and transmissivity are also considered as one of the most important parameters that describes the fluid motion in the aquifer. Transmissivity incorporates the total saturation thickness whereas hydraulic conductivity indicates unit one. Fetter defined the transmissivity as the following equation

$$T = Kh \tag{3.10}$$

where T is transmissivity (m^2/s), k is hydraulic conductivity (m/s), and h indicates the aquifer thickness (m).

3.2.4 Groundwater Flow

Field survey was conducted to locate the position of each borehole in the study area. The global positioning system (GPS) Garmin 64s was used to record the longitude, latitude and surface elevations with respect to the sea level at selected borehole locations within the study area. The static water level (SWL), or the depth of water level in the boreholes were measured using a dipper meter. The hydraulic head of the different borehole

locations were obtained by subtracting the depth to the water table in the boreholes from the ground elevation with respect to the sea level as shown in Equation (3.9).

$$HH = GE - SWL \quad (3.11)$$

HH= Hydraulic head (m)

GE= Ground Elevation (m)

SWL= Static Water Level (m)

Computer aided methods were adopted in this study to generate the base contour map and flow direction of the study area. The software package used for this work was SURFER by Golden Software. Groundwater level data was organized as XYZ files, where X and Y are plane coordinates of the measuring points and Z is a function of water table elevation.

3.2.5 Data/Model Input

Geographical Information Systems (GIS) technology was used extensively for processing raw data into GMS Modflow model datasets. The ArcGIS 10.7 software was used exclusively for GIS data manipulation and processing. The area's geology map was obtained from SamSam water website (https://www.samsamwater.com/maps/kenya/geology.php) and was digitized and used to identify the hydrogeologic features used to delineate boundaries in the model. A USGS digital elevation model (DEM) (National Elevation Dataset 2014) with a resolution of 30m of the area containing the ground-surface elevation data set was also processed for model importation. The conceptual model used ten (10) well locations and pump capacity data. A standard spatial referencing system was used to organize model data effectively, the WGS 1984 Universal Trans-Mercator (UTM) zone 36S.

A proper mathematical model representing the situation was chosen based on the conceptual model. A numerical method was then selected for which the mathematical

model was formulated. The numerical model used was the finite differences method. A computer program that could handle the numerical model used was GMS 10.4 with the application MODFLOW (Aquaveo, 2011a).

In the model design stage, the conceptual model was translated to a numerical form by converting conceptual stratigraphy to a computational domain in the form of a grid, for which the aquifer parameters, hydrologic stresses, boundary conditions, and initial water level were assigned. Input parameters employed in this study are horizontal hydraulic conductivities, recharge, and hydrostratigraphic units to establish the initial values for the model. Additionally, the following assumptions were made before the development of the model (Debbarma et al., 2016):

i. There is no confining material between the river and the aquifer.
ii. The influx into the system is mainly from recharge due to rainfall.
iii. The aquifer flow system is considered to be a steady-state.
iv. There are no evaporation losses into the aquifer.
v. The rainfall is uniform for the total period taken to run the model (average rainfall is considered here)

3.3 Determining the Flow System of Kericho Aquifer

3.3.1 Development and Construction of the Conceptual Model for the Study Area

A 3D conceptual model was built for this study to show the physical characteristics of the formations in the area. The conceptual modeling procedures in this study involved; (a) preparing the topographic model representing the surface conditions of the study area using ArcGIS, (b) constructing stratigraphic units based on borehole data, and then merging the surface and solid models. Interpolating between borehole data and solid model construction was done using Groundwater Modeling System (GMS). This began by constructing several cross-sections that helped in classification of the materials based on their hydraulic properties.

3.3.1.1 Defining Hydro-Stratigraphic Units

Defining the stratigraphic units is the first step in constructing the conceptual model. These units were converted into the hydrostratigraphic units by assigning hydraulic parameters obtained from pumping tests data. Stratigraphic location and elevation were obtained from geophysical reports of surveyed boreholes in the study area. The absolute elevation of each layer was obtained by subtracting the total thickness from the ground surface elevation of the well-head and were used to construct the 3D stratigraphic model and numerical model frame (Anomohanran et al., 2021). Based on the VES analysis, the area was characterized by same horizontal formation throughout the study area, interpolation between the stratigraphic units of boreholes provided the continuous surface for each horizon. Hydrostratigraphic units were defined by assigning hydraulic parameters obtained from pumping test and VES data (Hasan et al., 2021). In order to define the hydrostratigraphic units, one layer was considered as hydrostratigraphic unit by assigning horizontal hydraulic conductivity. The ground surface elevation data were obtained from DEM imported as a raster file to GMS as shown in Figure 3.4.

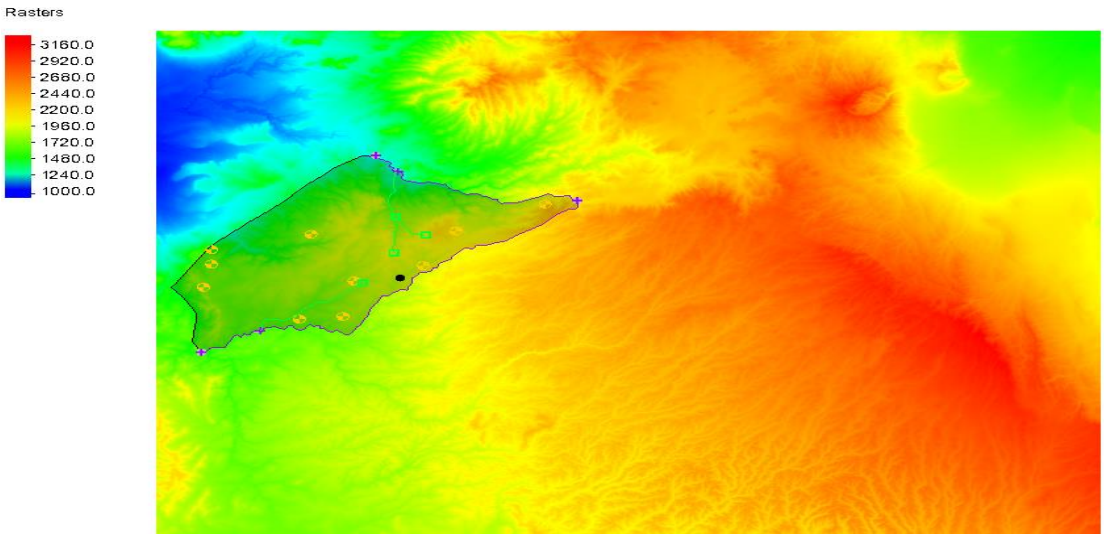

Figure 3.4: Top Layer Elevation Raster Clipped to GMS Model

3.3.1.2 Defining Groundwater Recharge and Discharge

Groundwater discharge occurs in the form of surface runoff and evapotranspiration. The aquifer system mainly discharges to streams, well abstractions and groundwater outflow (Barlow, 2012). An inventory of abstraction on production wells was recorded. Groundwater recharge can be defined as the water which infiltrates through the unsaturated zone and reaches the water table. Recharge package in GMS was used to simulate aquifer recharge due to infiltration and rainfall. Recharge is defined by specifying a recharge value for each stress period for each vertical column in the grid. Therefore, it is required to create recharge coverage to assign estimated values to the model which was assumed that the recharge in the study area was uniform. According to Pavelic et al. (2012), only 10% of the annual rainfall is recharged in Kenya's humid/sub-humid zones. The average annual rainfall in Kericho is 1925 mm; thus, the annual recharge **t**his translates to 0.0005 m/day. The recharge value obtained was then used for the steady state-run and the initial recharge rate during the steady-state calibrationn as shown in Plate 3.1

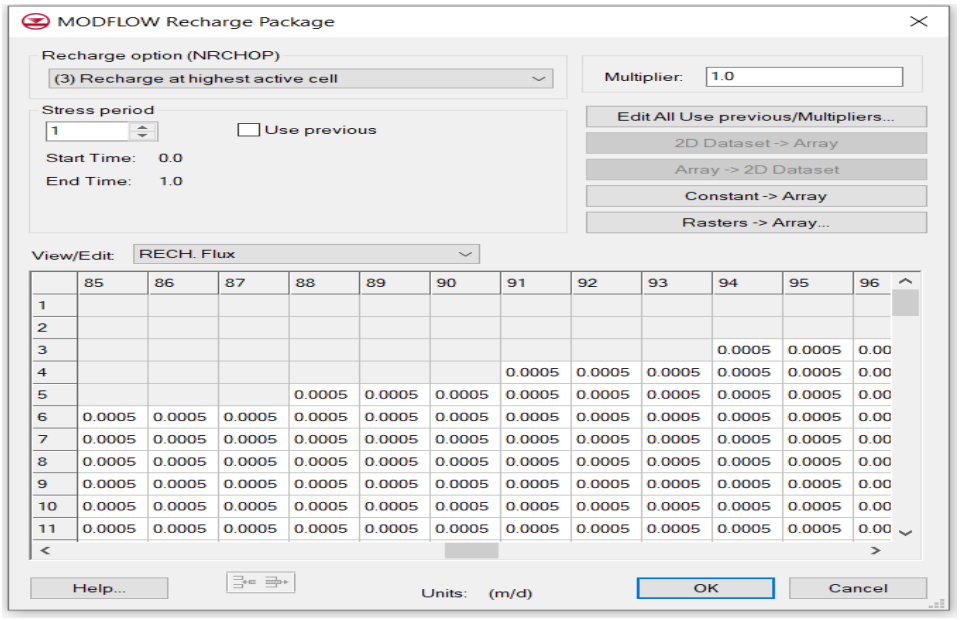

	85	86	87	88	89	90	91	92	93	94	95	96
1												
2												
3										0.0005	0.0005	0.00
4							0.0005	0.0005	0.0005	0.0005	0.0005	0.00
5				0.0005	0.0005	0.0005	0.0005	0.0005	0.0005	0.0005	0.0005	0.00
6	0.0005	0.0005	0.0005	0.0005	0.0005	0.0005	0.0005	0.0005	0.0005	0.0005	0.0005	0.00
7	0.0005	0.0005	0.0005	0.0005	0.0005	0.0005	0.0005	0.0005	0.0005	0.0005	0.0005	0.00
8	0.0005	0.0005	0.0005	0.0005	0.0005	0.0005	0.0005	0.0005	0.0005	0.0005	0.0005	0.00
9	0.0005	0.0005	0.0005	0.0005	0.0005	0.0005	0.0005	0.0005	0.0005	0.0005	0.0005	0.00
10	0.0005	0.0005	0.0005	0.0005	0.0005	0.0005	0.0005	0.0005	0.0005	0.0005	0.0005	0.00
11	0.0005	0.0005	0.0005	0.0005	0.0005	0.0005	0.0005	0.0005	0.0005	0.0005	0.0005	0.00

Plate 3.1: GMS Screenshot of Recharge in Kericho Study area

3.3.1.3 Constructing Land Surface Model

Digital elevation model (DEM) was used to define the upper boundary of the GMS model. DEM was represented as a raster in which each square has a specific elevation value. These elevation points are then interpolated in GMS to build a grid-based surface model representing the upper boundary of the model. Figure 3.5 shows the surface model of Kericho.

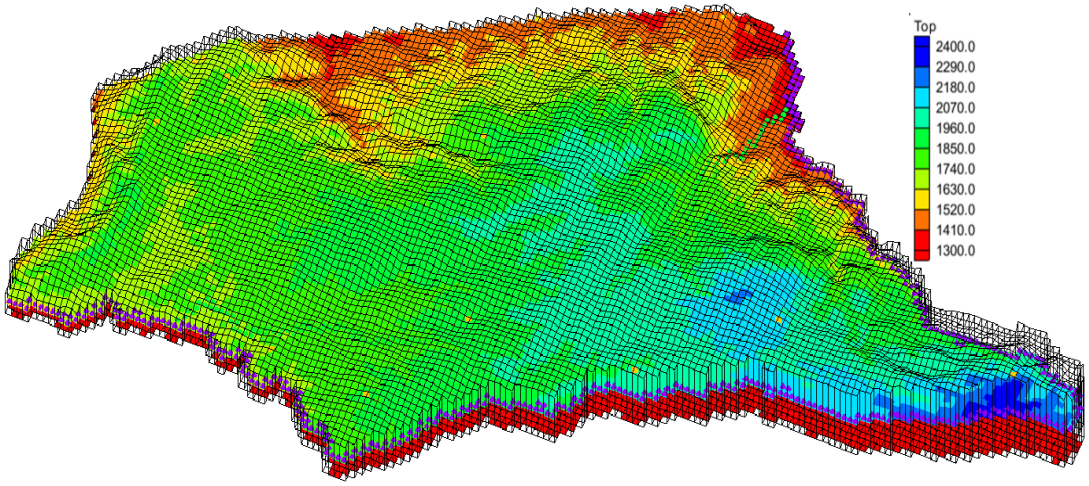

Figure 3.5: 3D View Land Surface Model of Kericho

3.3.1.4 Solid Model Development

A 3-D model was created incorporating geologic and hydrogeologic features. The solid model constructed was then converted into a grid model. Based on a study by Aberg et al (2019), this study also used data from ten boreholes, which is considered sufficient for constructing a solid model.

3.3.1.5 Boundary Conditions

The site specific knowledge acquired from the geology, topography and flow system in the area were used to establish the model boundaries. Physical boundaries such as impervious geologic formation, tight fault escarpments, topography and surface water

divides are used in defining the boundaries of the model domain. Dirichlet condition was used to represent a specified head boundary. The Neumann condition was applied to the flow rate across a boundary and also to prescribe an impermeable boundary.

The following boundaries were assigned along the perimeter of the active model domain: at the Eastern side boundary, there are no well-defined hydrologic or physical boundary conditions. Therefore, no flow boundary was assumed; the southern and western part represents Chemosit river and Kipchorian river, respectively; hence a general head boundary was used; along the northern side of the model domain, specified head boundary conditions were used, and the two rivers were represented using the drain package of MODFLOW. The drain package in MODFLOW needs three parameters: (i) river stage, (ii) river bed elevation, and (iii) conductance of the riverbed material (Boel, 2008).

Field investigations delivered average values for river water level h = 9.6 m and river depth d = 1.2 m. The conductance of the river sediments C = 2.66 m^2 /d was calculated using Equation 3.10 given as:

$$C = KA/b \tag{3.12}$$

Where

K = hydraulic conductivity of the bottom sediments (m/d)

A = surface area of the bottom sediments (m^2)

b = thickness of the sediment layer (m)

A more extensive description of the applied groundwater model and its internal and external boundary conditions can be found in Touchant et al. (2007). In the vertical direction, the model is bounded by a recharge flux at the top and an impermeable soil layer at the bottom.

3.3.2 Numerical Modelling Procedure

A 3-D conceptual model was built for this study to show the physical characteristics of the formations in the area. The conceptual modeling procedures in this study involved; (a) preparing the topographic model representing the surface conditions of the study area using ArcGIS, (b) constructing stratigraphic units based on borehole data, and then merging the surface and solid models. Interpolating between borehole data and solid model construction was done using Groundwater Modeling System (GMS). This began by constructing several cross-sections that helped classify the materials based on their hydraulic properties.

3.3.2.1 Model Design

Each shapefile and raster dataset was brought into GMS, converted to coverage, and mapped in the MODFLOW model. These coverages were as follows; the model extents, hydraulic properties, sources and sinks (boundary head conditions, drains, wells), and recharge rates shown in Figure 3.6.

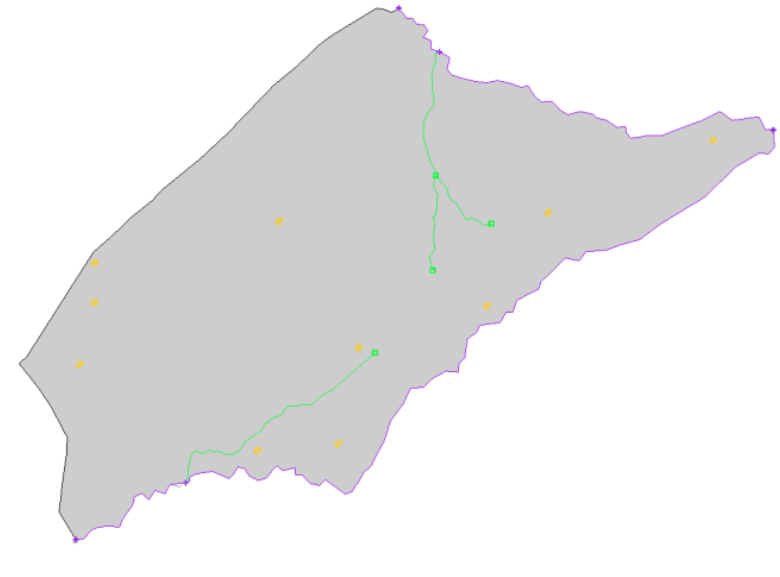

Figure 3.6: GMS Interface with all Coverages Mapped

Coverages were mapped in the MODFLOW grid cells to add data to the model. Coverages are grouped under conceptual models (Aquaveo, 2019). The model outline coverage was set to the extent of the MODFLOW model, and the active cells used were created based on the outline shape. The MODFLOW grid was made with 300m wide cells in the x and y directions and one vertical layer going downwards. The elevation raster datasets were mapped in the cells, as shown in Figure 3.7.

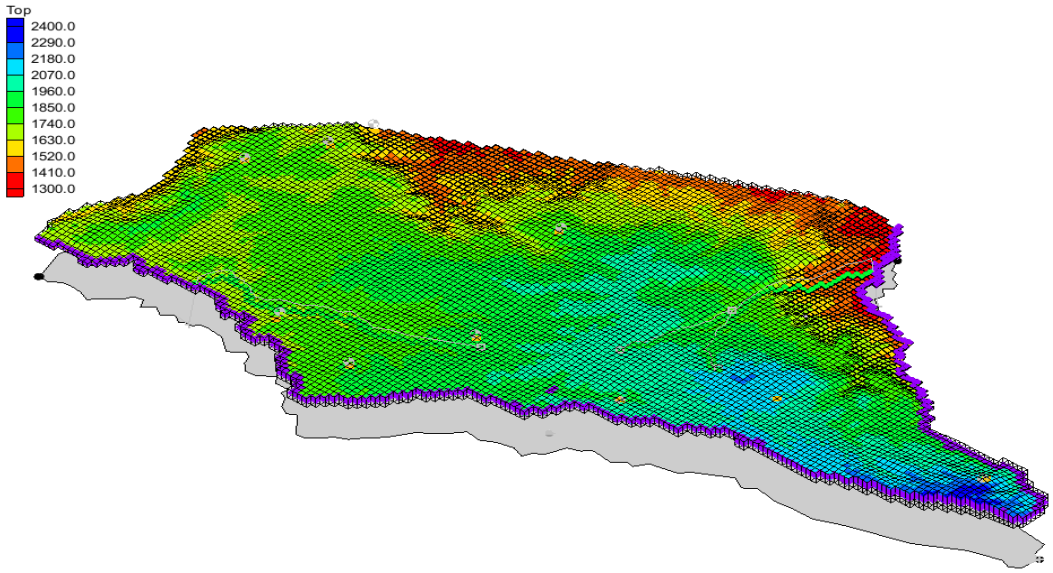

Figure 3.7: 3D GMS MODFLOW Model Display with Top of Cell Elevation Values (m)

The total number of active cells was 8,494. The model grid was rotated by 14.7 degrees towards the northeast. Table 3.1 represents the properties of the grid model designed in this study.Once all the coverages were mapped, and all the data was entered into the MODFLOW model, the model was run. Head values from this model were calculated at every time step, or in this case, day shown in Figure 3.8

Table 3.1: Properties of the Designed Grid Model

Item	Value	Units
Grid type:	Cell Centered	
X origin:	726656.87890288	(m)
Y origin:	9942762.1160323	(m)
Z origin:	353.0706	(m)
Length in X:	52419.693130723	(m)
Length in Y:	29967.974920337	(m)
Length in Z:	1412.706	(m)
Rotation angle:	14.6747	
AHGW X origin:	719065.06768965	(m)
AHGW Y origin:	9971752.5269181	(m)
AHGW Z origin:	1765.7766	(m)
AHGW Rotation angle:	75.3253	
Minimum scalar:	1351.033	
Maximum scalar:	2116.657	
Num cells i:	100	
Num cells j:	175	
Num cells k:	1	
Number of nodes:	35552	
Number of cells:	17500	
No. Active cells:	8494	
No. Inactive cells:	9006	
Projection:	UTM, Zone: 36, WGS 1984, meters	
Projection:	UTM, Zone: 36, WGS 1984, meters	

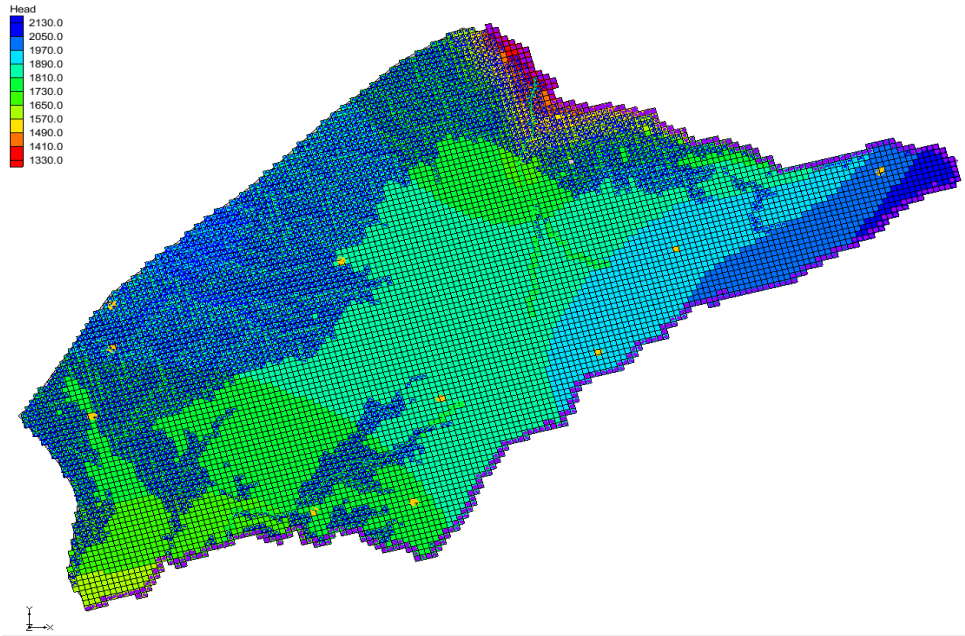

Figure 3.8 : Simulated Model Head Values (m)

3.3.2.2 Governing Equation

The main focus of the study was to understand the groundwater flow system; therefore, the selected model was MODFLOW. The code is based on Darcy, and mass continuity flow partial differential equation (Anderson & Woessner, 1992) given as Equation 3.11:

$$\frac{\partial}{\partial x}\left(k_{xx}\frac{\partial h}{\partial x}\right)+\frac{\partial}{\partial y}\left(k_{yy}\frac{\partial h}{\partial y}\right)+\frac{\partial}{\partial z}\left(k_{zz}\frac{\partial h}{\partial z}\right)-W=S_s\frac{\partial h}{\partial t} \quad (3.13)$$

Where,

kxx, kyy, kzz = Hydraulic conductivity along x, y, and z coordinate axes (LT-1)

h = Potentiometric head (L),

W = Flux per unit volume representing sources and sinks of water (T-1),

S_s = Specific storage of the porous material (L-1), and

t = Time (T)

This study assumed a steady state numerical simulation; therefore, no change in storage with time, and hence the right-hand side of the Equation was set to zero. The modeling process was developed using GMS (Groundwater Modeling System) software v. 10.4, which supports MODFLOW as a pre and post-processor.

3.3.2.3 Dimensional Approach

A 3-D approach also provides a closer description of reality; therefore, the 3-D method was chosen for this project. Furthermore, daily groundwater pumping was done on individual wells; hence, the storage term was considered constant. Accordingly, the modeling was limited to the steady state condition.

3.3.3 Model Calibration, Validation, Simulation and Sensitivity Analysis

3.3.3.1 Calibration

During calibration, also known as the Parameter Estimation Process, a fine-tuning of the parameters was done so that the model could simulate heads that match the measured field values (Tziatzios et al., 2021). The parameter estimation process was carried out using the calibration program PEST. Calibration based on heads of water along the stream was done by choosing several locations along the stream to measure the head of water using Google Earth image and then compared with the heads computed by the model. Both computed and actual heads were plotted to determine the correlation coefficient. The Root Means Square Error (RMSE) presented as Equation 3.8 was used to determine the most optimal balance between the observed and the computed heads.

$$RMSE = \sqrt{\frac{E(M-C)^2}{N}} \quad (3.14)$$

Where:

M = Measured values,

C = Computed values and

N = Number of observation wells.

3.3.3.2 Simulation

The MODFLOW packages used in the MODFLOW simulation are specified in the Packages dialog. Some packages are required for a simulation, and some are optional. One of the flow model packages and one of the solver packages must be selected. The technique to discretize the spatial domain is called the Layer Property Flow (LPF). The approach specifies properties controlling flow between cells. After the MODFLOW grid and Elevation were set, MODFLOW was set to Steady State model and 2005 Version with Layer Property Flow package. The optional packages Time-Variant Specified Head (CHD), Drain (DRN), Well (Well1), and Recharge (RCH) were activated as shown in Plate 3.2

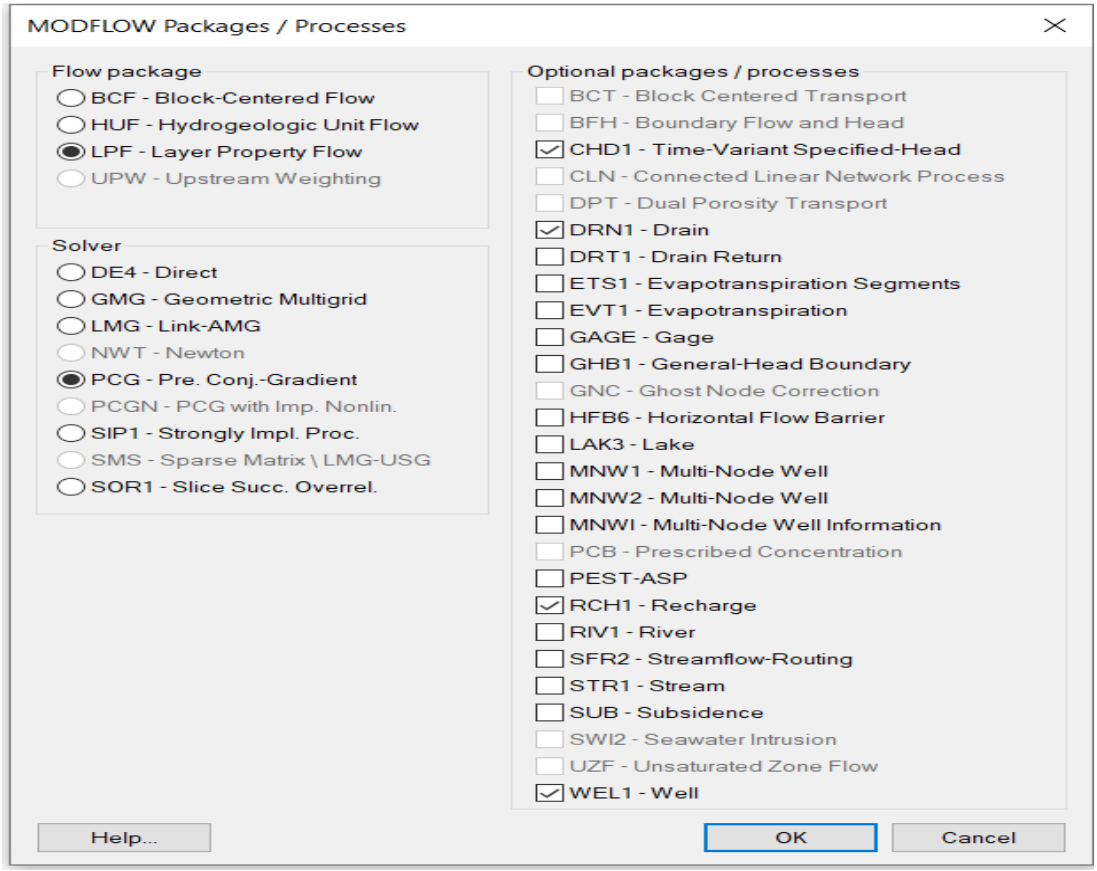

Plate 3.2: MODFLOW Packages Used for Groundwater Simulation

The Time-Variant Specified-Head package simulates specified head boundaries that can change within or between stress periods. The boundary coverages were mapped in MODFLOW under the CHD package. The CHD package works by assigning a specific head value to each cell and the stress period defined. These values were set before running the MODFLOW model run. Additionally, the starting heads for MODFLOW were placed at the top Elevation for layer 1 to ensure no errors occurred in the first stress period.

The Drain Package was used to determine the drain-water infiltration in the aquifer system. The drain inputs were located in sources and sink coverage, which were then mapped to the DRN package. The Drain package (DRN) is used to simulate the effect of drains on an aquifer. Drains remove water from the Aquifer as long as the water table is

above the Elevation of the drain. If the water table falls below the Elevation of the drain, the drain has no effect. Therefore, the removal rate is proportional to the difference in elevation between the water table and the chute. The constant of proportionality is the conductance of the fill material surrounding the drain (http://aquaveo.com).

The Well Package was used to determine the flow rate (m^3/day) of the wells in the area. The well coverage consisted of 10 wells. The screen elevations (m), well radius (m), and daily well flows (m^3/d) were all input into the coverage. The wells were mapped in MODFLOW, and the well was located under the Wel 1 package.

The Recharge Package (RCH) was used to determine the groundwater recharge in the Aquifer from the direct infiltration of rainfall. First, recharge rates (m/d) were inputted for the study area. To do this, the shapefile was converted to the recharge coverage, and then a polygon was drawn around the recharge basin. Next, the recharge rates were mapped to the MODFLOW model under the RCH package. The RCH package works by applying the recharge rate (m/day) to the top area of the cell (m^2) to get a recharge volumetric inflow (m^3/d) for each cell with a defined recharge (Aquaveo, LLC, 2019). The Preconditioned Conjugate Gradient (P.C.G2) was selected as the Solver Package.

3.3.3.3 Validation

The remaining data during calibration was used to validate the model.

3.3.3.4 Sensitivity Analysis of MODFLOW Model

The sensitivity analysis was done using the Automated Sensitivity analysis option in GMS MODFLOW. The sensitivity approach was performed using a systemic change in the Aquifer's value of recharge and hydraulic conductivity.Dimensionless composite scaled sensitivities were calculated for each parameter using scaled sensitivities.

3.4 Stress Conditions Scenarios

The calibrated groundwater flow steady-state model was used to examine how the groundwater flow system would respond to changes in water management and hydrologic conditions in the Kericho Aquifer. To understand the prospects of groundwater and also to provide a vision for the decision-makers to use groundwater in a manner that does not harm the environment and can still be available for future use, three scenarios were examined as shown in Table 3.2

Table 3.2: Different Scenario Types

Scenario no.	Type of Scenario	Justification
1.	Pumping rates were increased in the study area, and the model was simulated with 10% increment of discharge values.	Examining increasing pressures on water resources due to population growth
2.	Reducing the constant head by 5m, reducing recharge and pumping rate by 25% and 50%, respectively	Examine resilience to climate change
3.	Decreasing the constant head by 5m, reducing recharge by 25% and pumping rate up to 50%.	Examine the effect of both increase in population pressure and Climate change

CHAPTER FOUR

RESULTS AND DISCUSSION

4.1 Electrical Resistivity and Underlying Geology

The VES analysis shows that the area is characterized by 4 to 5 geoelectric subsurface layers, with 4 - layer types occurring widely. Moreover, the aquifer resistivity in the study area was found to range between 12 and 5,918 Ωm, with an average of 610 Ωm. The minimum resistivity was observed at VES 27, while the maximum resistivity was observed at VES 38. The summary of the interpreted electrical resistivity survey and geology, aquifer resistivity and thickness of the study area is presented in Appendix 1.

The spatial distribution of the aquifer thickness is shown in Figure 4.1

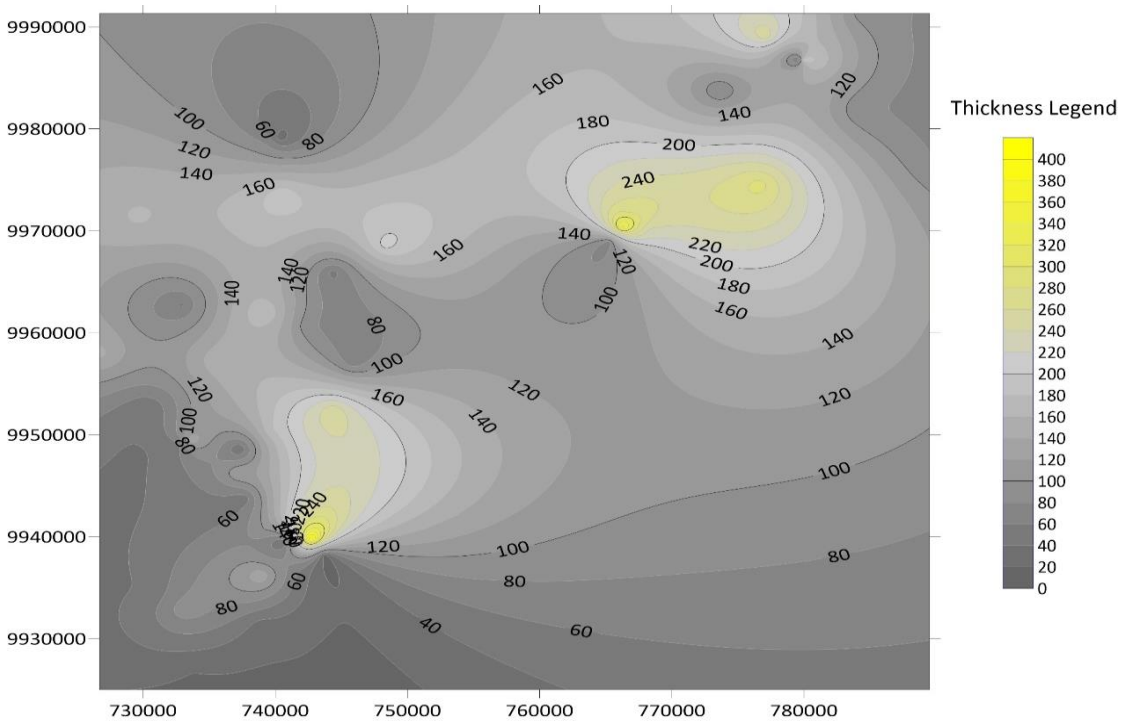

Figure 4.1: Spatial Distribution of Aquifer Thickness

The minimum value was observed at point VES 13/51, a maximum value at point VES 48, and an average depth of 118m. It was observed that the aquifer thickness is high in the Northeastern and southwestern parts of the study area, as summarized in Table 4.1.

Table 4.1: Aquifer Thickness

	Thickness (m)		
Zone/Aquifer	**Range**	**Average**	**SD**
Belgut	54-256	136.67	79.22
Bureti	15.1-404.7	85.78	103.52
Kipkelion	44-289	145.19	81.68
Soin/Sigowet	26-208	98.65	63.65

The spatial distribution of aquifer resistivity in the study area is shown in Figure 4.2 shows

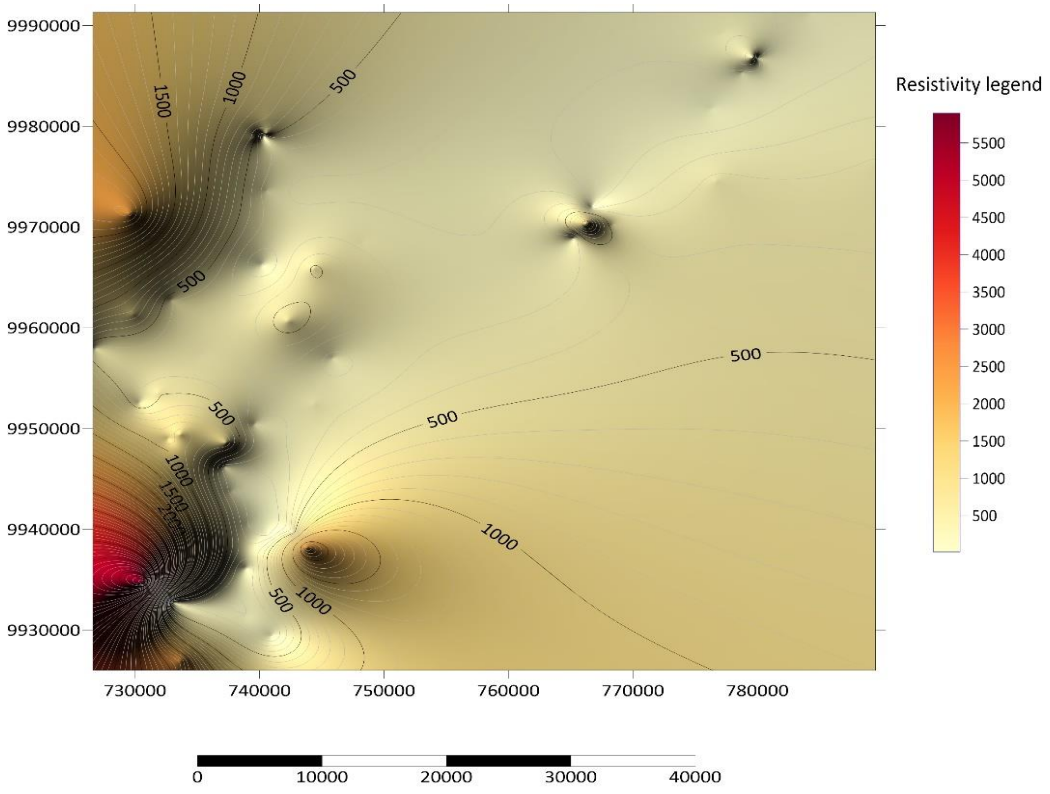

Figure 4.2: Spatial Distribution of Aquifer Resistivity

The highest value of spatial distribution of aquifer resistivity was observed in the southwestern part (Bureti) with an average of 976.9 Ω, and the lowest in the North Eastern part (Kipkelion) of the study area, which has an average of 376.75 Ω (Table 4.1). According to Abidin et al. (2012), high resistivity values indicate a low conductive zone, while a low resistivity value is always assumed to be a highly conductive zone, which reflects a weak zone that commonly contains water. As such, it can be deduced that ves stations in the Kipkelion area has a great potential for groundwater, owing to the low values of aquifer resistivity and high conductive geomaterials.

It was observed that most parts of the watershed are characterized by low hydraulic conductivity. Figure 4.3 shows the Spatial Distribution of Hydraulic Conductivity across the study area. Hydraulic conductivity determines the rate at which water can flow into and through porous storage rocks in aquifers. Therefore, areas with high hydraulic conductivity will likely have good aquifer recharge capability. The variability in the hydraulic properties mainly results from the intense fracturing and heterogeneity due to the presence of phonolites. Hydraulic parameters from an aquifer test can be used as good indicator of the quantity of water that can be abstracted from an aquifer.

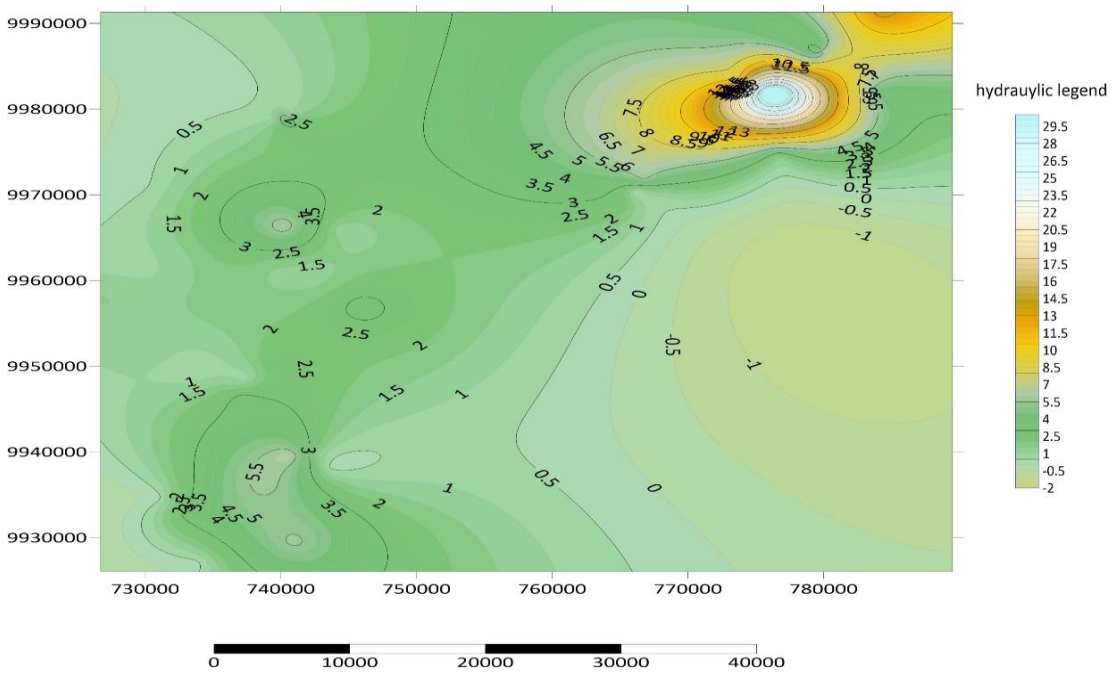

Figure 4.3: Spatial Distribution of Hydraulic Conductivity

4.2 Aquifer Hydraulic Parameters from Pumping Test Data

The results in Table 4.2 show that the calculated specific capacity of the wells ranged between 0.34 and 125.84m^3/d/m, with a mean of 15.02m^3/d/m (Table 4.2). Further, hydraulic conductivity varied between 4.4*$10^{\wedge-4}$m/d (Chepngobob) and 11.1m/d (Kaptaragon). From the mean values of hydraulic parameters (T= 38.39 m^2/d, K = 0.57 m/d, SC = 15.02 m^3/d/m), it is evident that the Kericho aquifer has substantial quantity of water. The results further reveal that Kaptaragon has the highest hydraulic parameters and the most productive borehole (SC = 125.84 M^3/d/m).

Table 4.2: Aquifer Hydraulic Characteristics Values Calculated from Cooper-Jacob's Straight Line Equation

S/No.	Borehole Name	Yield	T(m^2/day)	Range	Class Type	Hydraulic Conductivity(m/day)	Specific capacity(m^3/d/m)
1	Tapsabei Korir	4.32	1.73	1 - 10	Low	0.02	4.98
2	Ronald Cheruiyot	1.80	0.44	0.1 - 1	Very low	0.00	0.50
3	Evergreen Tea Factory Ltd	2.00	0.36	0.1 - 1	Very low	0.02	0.34
4	Chepkemel Primary School	5.54	0.68	0.1 - 1	Very low	0.01	1.38
5	Chepngobob Pri	7.00	0.32	0.1 - 1	Very low	0.00	11.43
6	Chebwagan	1.20	0.03	0.1 - 1	Very low	0.00	1.28
7	Cheres	10.00	1.24	1 - 10	Low	0.01	32.83
8	Kabokyek	4.10	0.57	0.1 - 1	Very low	0.02	1.15
9	Kamuingi	2.50	1.62	1 - 10	Low	0.03	1.81
10	Kapcheluch	6.00	17.20	10 - 100	intermediate	0.20	11.84
11	Kapkatet Hospital	4.30	0.04	0.1 - 1	Low	0.00	1.63
12	Kaproret	6.00	2.62	1 - 10	Low	0.02	3.52
13	Kaptaragon	9.70	728.00	100 -1000	High	11.10	125.84
14	Katet	7.00	135.00	100 -1000	High	1.77	125.37
15	Kiboet	1.70	1.36	1 - 10	Low	0.04	2.25
16	Kibugat	3.10	1.18	1 - 10	Low	0.01	1.69
17	Kipsitet	6.00	0.94	0.1 - 1	Very low	0.10	2.01
18	Leldet	5.30	0.67	0.1 - 1	Very low	0.01	1.39
19	Lemotit	0.70	2.25	1 - 10	Low	0.10	2.71
20	Londiani	4.00	1.30	1 - 10	Low	0.01	1.28
21	Motero	6.00	11.40	10 - 100	intermediate	0.11	10.84
22	Seretet/Cheptororiet	1.90	0.57	0.1 - 1	Very low	0.00	0.57
23	Sigowet Hospital	3.50	1.43	1 - 10	Low	0.03	1.73
24	Soliat	6.00	10.50	10 - 100	intermediate	0.10	12.04
	Average		**38.39**			**0.57**	**15.02**

Michael (2006) reported that the storage coefficient (S) for unconfined aquifer types should be within a range of 0.1 and 0.3. To evaluate S, the observation distance well is required, however, in this study, S could not be calculated since no observation wells were used. The productivity of a well is often expressed in terms of its specific capacity (Freeze & Cherry, 1979). As such, in this study, the specific capacity was calculated to understand the productivity of the Kericho aquifer.

The interpreted results show that the Kaptaragon borehole is the most productive (SC = 125.84 $M^3/d/m$, T = 728 m^2/d) compared to boreholes in other locations within the study area. Based on standard values by Kransy (1993), the average value computed for the area can generally be categorized as having intermediate potentials for groundwater transmission and groundwater withdrawal of local water supply.

4.2.1 Determination of Yield

The highest yield value from the pumping test was 10 M^3/hr (Cheres), while the lowest was 0.7 M^3/hr (Lemotit). As detailed in Table 4.3, the various boreholes studied had varying yields across the study area.

Table 4.3: Results for the Borehole Yield

S/No	Borehole Name	Yield (m^3/hr)	Borehole radius (m)	Casing radius (m)
1	Tapsabei Korir	4.32	0.075	0.11
2	Ronald Cheruiyot	1.8	0.075	0.11
3	Evergreen Tea Factory Ltd	2	0.075	0.11
4	Chepkemel Primary School	5.54	0.075	0.11
5	Chepngobob Pri	7	0.075	0.11
6	Chebwagan	1.2	0.075	0.11
7	Cheres	10	0.075	0.11
8	Kabokyek	4.1	0.075	0.11
9	Kamuingi	2.5	0.075	0.11
10	Kapcheluch	6	0.075	0.11
11	Kapkatet Hospital	4.3	0.075	0.11
12	Kapkisiara	4	0.075	0.11
13	Kaptaragon	9.7	0.075	0.11
14	Katet	7	0.075	0.11
15	Kiboet	1.7	0.075	0.11
16	Kibugat	3.1	0.075	0.11
17	Kipsitet	6	0.075	0.11
18	Leldet	5.3	0.075	0.11
19	Lemotit	0.7	0.075	0.11
20	Londiani	4	0.075	0.11
21	Motero	6	0.075	0.11
22	Seretet/Cheptororiet	1.9	0.075	0.11
23	Sigowet Hospital	3.5	0.075	0.11
24	Soliat	6	0.075	0.11

4.2.2 Static Water Level and Drawdown

Static water levels from non-pumping boreholes ranged between 10 m and 151.54 m, with a mean value of 56.88 m. Drawdown values obtained after the pumping test of the boreholes ranged between 1.34 m and 142.3 m. The least drawdown value was recorded in one of the boreholes in Chebwagan, while the highest yield was recorded at Katet. Both the static water level and drawdown parameters depend on the permeability of the aquifer and recharge. The more permeable an aquifer is, the more recharge it will record, hence a lesser drawdown in the well. The average drawdown value of 41.1 m indicates

that the aquifers in the area are efficient in recharge and discharge, owing to good permeability.

4.2.3 Groundwater Flow Direction

The direction of groundwater movement is influenced by the level of groundwater. Moreover, discharge is typically highest in areas where the groundwater level is lowest (Egbai et al., 2013). The results suggest land use activities such as solid waste disposal in the region will be unfavorable for communities within the study area's western region. Hence, knowledge of groundwater flow is essential in choosing a dumpsite location. Figure 4.5 shows the various trends in the flow direction within the study area.

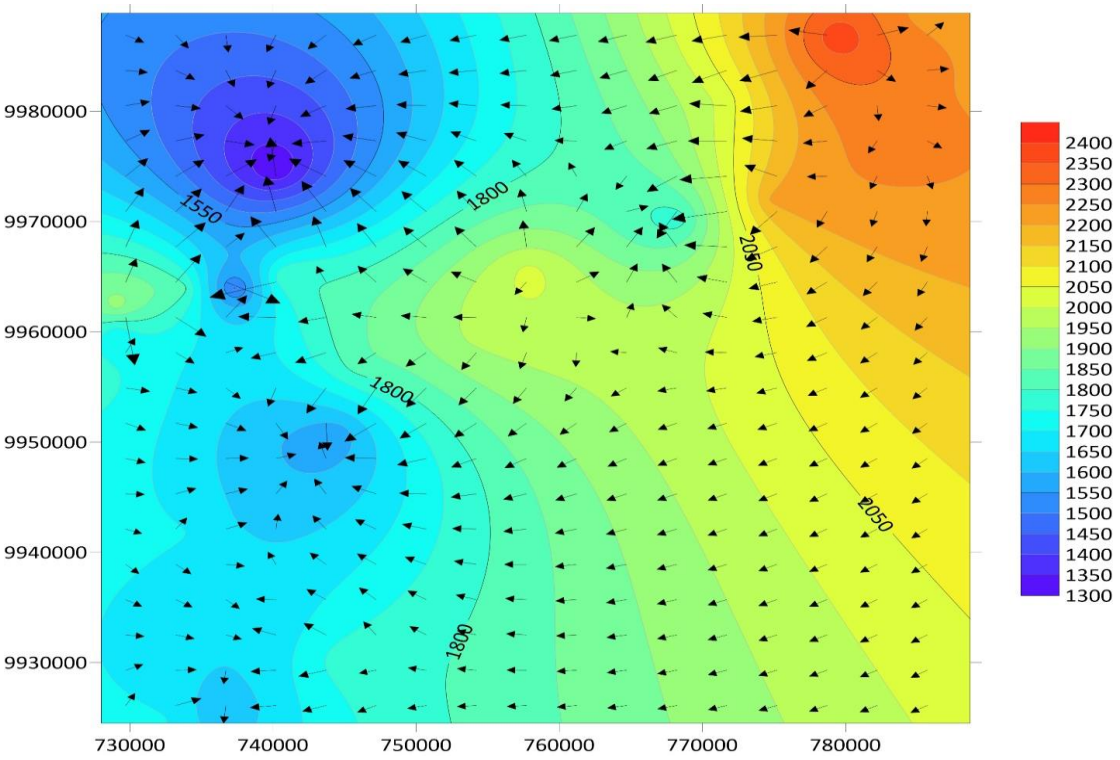

Figure 4.4: Groundwater Flow Direction Map in Kericho

4.2.4 Empirical Relationship

Regarding the hydraulic conductivity, Figure 4.5 demonstrates the close relationship between both hydraulic conductivity calculated from the Pumping test (water wells) and VES technique. The corresponding empirical correlation can be written as

$$K_{well}=-0.0291(K_{ves})^2 + 1.0189K_{ves} + 0.1762 \quad (4.1)$$

Where k_{Well} and k_{VES} are the hydraulic conductivity gained from the Pumping test (water wells) and VES technique, respectively. Similar to the porosity, as the hydraulic conductivity of the rock increases, the value of the hydraulic conductivity estimated by the VES technique becomes closer to the water wells' results.

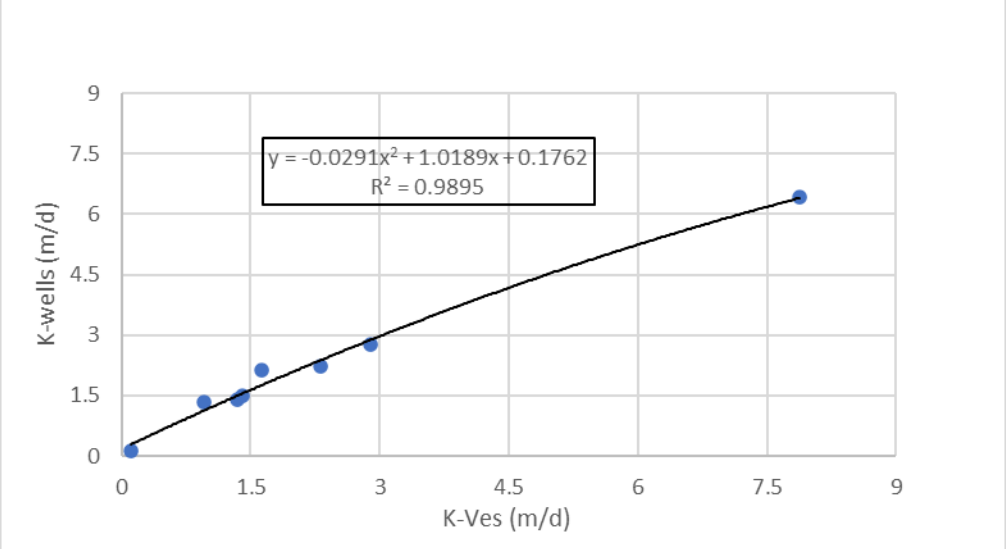

Figure 4.5: Hydraulic Conductivity Calculated by Pumping Wells vs Ves Technique

4.3 Model Calibration

Hydraulic conductivity ranged from 0.279 m/d to 1.12 m/d, indicating that the area is dominated by coarse and fine sand. The highest value for hydraulic conductivity was recorded in Soin (1.12 m/d), while the lowest was recorded in Kipkelion (0.279 m/d) as shown in Table 4.4.

Table 4.4: Calibrated Hydraulic Conductivity and Recharge for each Zone

Description of the Zone	Parameter code	Value (m/d)
Hydraulic Conductivity of Soin	HK_21	1.12
Hydraulic Conductivity of Ainamoi	HK_55	0.619
Hydraulic Conductivity of Belgut	HK_196	0.956
Hydraulic Conductivity of Kipkelion	HK_62	0.279
Recharge for all the zones	RCH_5	0.00022

**HK_x represents the model parameter code with the number as a unique identifier(x)*

High hydraulic conductivity values have been associated with soil texture (Sule & Ayenigba, 2017). For example, Quitaneg (2021) recorded a hydraulic conductivity of 41.80 m/d, suggesting that the region was dominated by medium-grained to coarse-grained sand. In a related study, Sule and Ayenigba (2017) reported a hydraulic range of between 0.1 and 2.9 m/d for the steady-state calibration. In the same study, Sule and Ayenigba (2017) recorded a recharge value of 0.0001 m/d.In general, good relationships were found between observed and simulated groundwater levels, and the average absolute difference between them was 0.41m shown in Table 4.5.Similar results were recorded in a study conducted by Quitaneg (2021), where the difference between the observed and simulated values was small.

Table 4.5: Modflow Simulation Results during Calibration

Observation point	Observed Value(M)	Simulated Value(M)	Residual Head(M)
H_1	1681	1681.9885	-0.9885
H_2	1706	1706.012	-0.012
H_3	1852	1852.3292	-0.3292
H_4	1359	1360.717	-1.717
H_5	1441	1440.1469	0.8531
H_6	1664	1664.1656	-0.1656
H_7	1778	1778.14	-0.14
H_8	1877	1877.3401	-0.3401
H_9	1882	1882.5823	-0.5823
H_{10}	1686	1686.0164	-0.0164
H_{11}	1692	1692.8846	-0.8846
H_{12}	1710	1709.6191	0.3809
H_{13}	1717	1716.826	0.174
H_{14}	1766	1766.1014	-0.1014
H_{15}	1781	1780.9641	0.0359
H_{16}	1803	1803.1989	-0.1989
H_{17}	1823	1823.3201	-0.3201
H_{18}	1835	1834.6127	0.3873
H_{19}	1848	1848.9122	-0.9122
H_{20}	1374	1373.4252	0.5748
H_{21}	1409	1409.1455	-0.1455
H_{22}	1553	1552.9651	0.0349
H_{23}	1617	1616.6779	0.3221
H_{24}	1724	1723.5665	0.4335
H_{25}	1833	1832.874	0.126
H_{26}	1880	1880.4618	-0.4618

The absolute difference between the observed and computed head values (Residual head) ranged from 0.8531 to 1.717m. This variance demonstrates a relatively good agreement between the observed and the calculated values (Figure 4.5). The small variance between the computed and observed values can be attributed to model calibrated, which led to minimal errors during the model run. The existing errors were probably caused by the effect brought about by the boundary conditions.

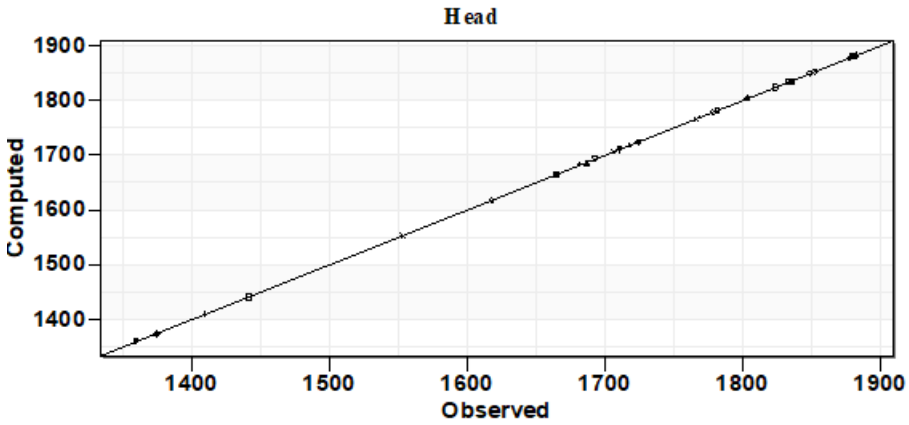

Figure 4.6: Computed head (m) Plotted against Observed head (m)

The computed and observed heads are within a straight line, indicating that the model used was of good fit (Quitaneg, 2021). Furthermore, the RMSE was used to determine the optimal balance between the observed and computed heads. The observed head calibration target of ±1m was used. As a result, an RMSE of no more than 1m was considered acceptable for the calibrated model. The calibration had an RMSE value of about 0.56m. This reasonably agrees with the observed and computed head values, with a calibration target of within ±1 m. Therefore, we can conclude that all the parameters calculated for the aquifer system's hydrogeological, hydrological, and hydraulic characteristics, then applied in the MODFLOW model approach, depict actual field conditions. Table 4.6 presents the water budget of the calibrated model, while the groundwater head distribution is shown in Figure 4.6:

Table 4.6: Model Flow Budget for Steady State Conditions

Contributing Parameter	IN (m^3/day)	OUT (m^3/day)
Storage	0	0
Constant Head	730,299	1,152,102
Wells	0	104
Drains	0	195,231
Recharge	618,084	0
TOTAL IN=	1348,383	-1,348,373
IN-OUT=		-0.01
PERCENT DISCREPANCY		0.00

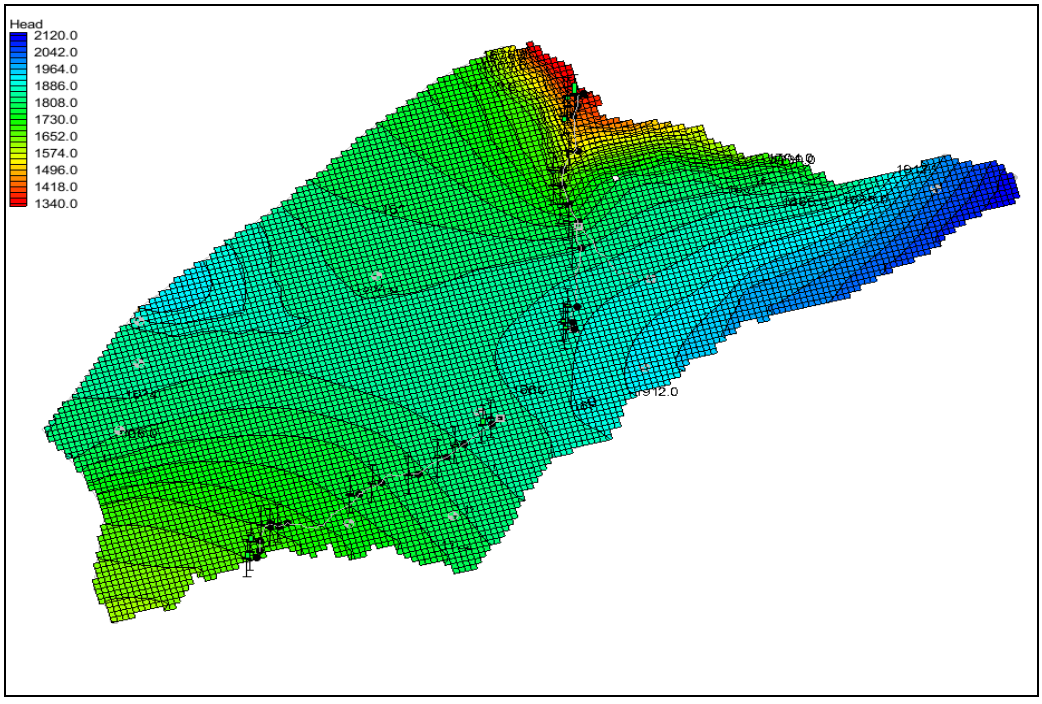

Figure 4.7: Steady State Groundwater Head Distribution Layer (m)

Analysis shows that the model's inflows from direct infiltration of rainfall (Recharge) and infiltration through torrent beds (Constant Head) are $13.48383x10^2$ M^3. At the same

time, the outflows from pumping well drains and groundwater outflows in part of the model (Constant Heads) are $13.48373x10^2$ m^3. Thus, there is an equilibrium between the inflows and the outflows, which is very significant during groundwater simulation.

A verification run was done for the model. This run used the calibrated parameters for the model and then was checked against the observed head values. Although there are still differences between the model and the observed values, these differences are acceptable based on the available data. Therefore, it can be said that the calibrated model generally represents the groundwater basin at Kericho, and the results are considered satisfactory.

4.3.1 Sensitivity Analysis

Results for sensitivity analysis are shown in Figure 4.7 which indicate that recharge rate was the most sensitive parameter analyzed, followed by the Kx-value of Belgut, Ainamoi, Soin, and Kipkelion.

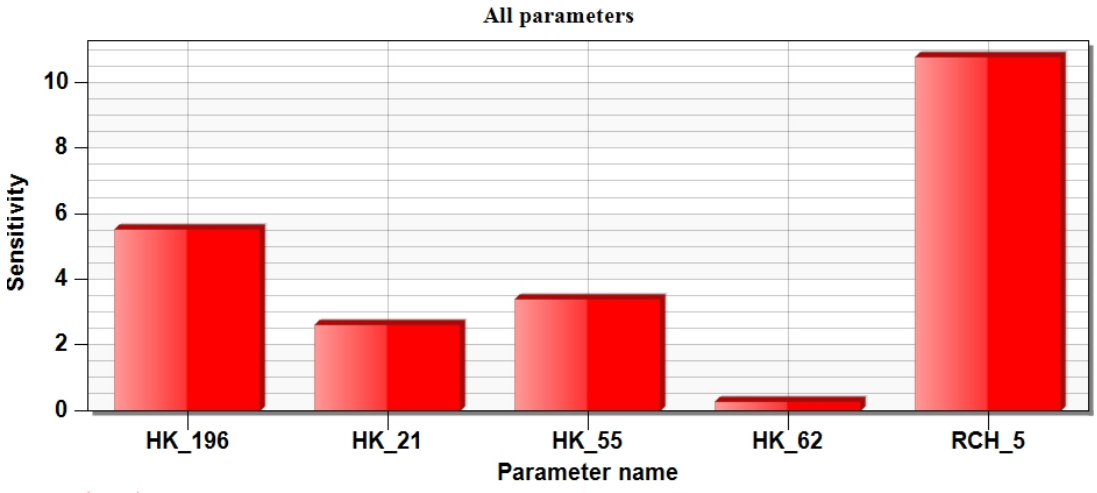

Figure 4.8: Composite Scaled Sensitivities vs. Selected Parameters

From the analysis, the model was sensitive to recharge and hydraulic conductivity. Similar results were reported by Sule and Ayenigba (2017) in Nigeria. Recharge rate

was the most sensitive parameter analyzed, followed by the Kx-value of Belgut, Ainamoi, Soin, and Kipkelion, respectively (Figure 4.8). Therefore, a slight change in the recharge rate would affect the results obtained from the model calibration (Sule & Ayenigba, 2017).

Further, the analysis established that a change in either hydraulic conductivity or recharge would affect the results obtained from model calibration. The results are in agreement with the findings of Foster and Maxwell (2019) in a study conducted in Colorado River catchment in the United States. The authors (Foster & Maxwell) reported that recharge and hydraulic conductivity were the most sensitive parameters during the calibration of the GMS-MODFLOW model.

4.4 Predictive Scenarios

4.4.1 Scenario 1

Scenario 1 results show that there was a minimal decrease in the level of groundwater near the drains and rivers. This can be attributed to the water transfer from the river to the aquifer. This is because additional groundwater discharge increases river-water seepage into the connected aquifers. This shows that a gradual rise in the groundwater pumping increases river seepage to the aquifer, as shown in Table 4.7.

El-Rawy et al. (2021) reported that groundwater discharge increases river-water seepage into the connected aquifers. This demonstrates that a slow increase in the amount of groundwater being pumped results in an increase in river water entering the aquifer.

Table 4.7: MODFLOW Water Budget Results for Scenario 1 after Increasing the Pumping Rate by Some Percentage

Percentage Reduction	Pumping Rate (m^3/day)	River leakage in (m^3/day)	River leakage out (m^3/day)	River In-Out
0	1040.16	89040.0	180415.0	-91375.0
10	1144.176	89063.6	180368.6	-91305.0
20	1248.192	89087.2	180321.8	-91234.6
30	1347.17	89109.1	180277.8	-91168.7
40	1473.1799	89140.5	180216.3	-91075.9
50	1560.24	89158.1	180181.4	-91023.4

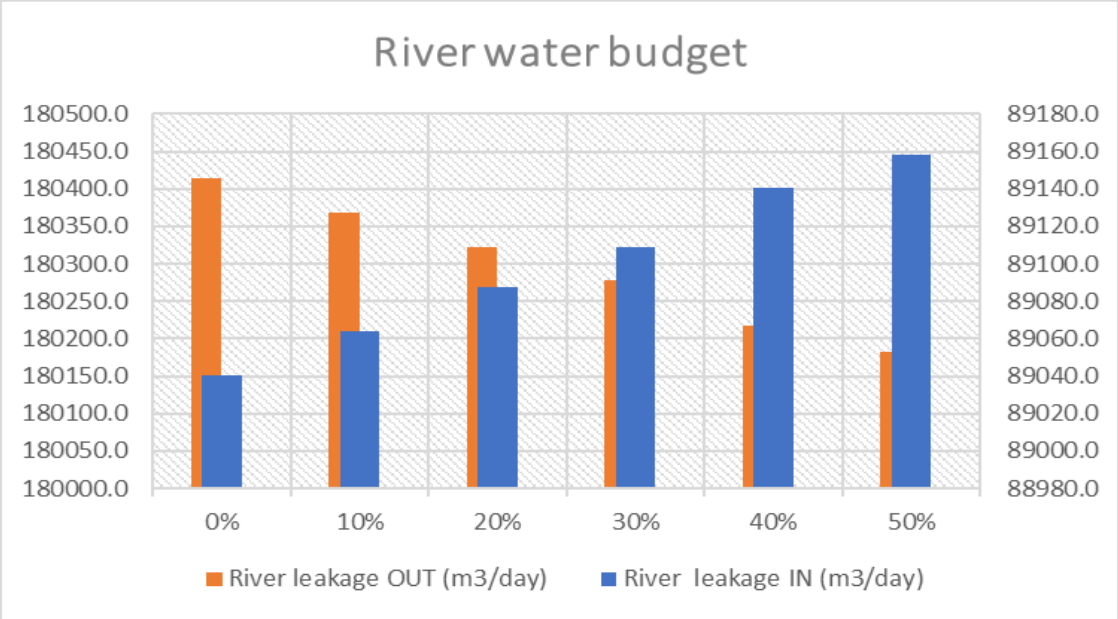

Figure 4.9: The Relation between the Percentage Increase of the Pumping Rate and the River Leakage IN and OUT of Aquifer after Keeping the Recharge Constant

From the study findings, when there is no pumping from the groundwater aquifer, the river gains about 180,000 m^3/day of water. Accordingly, increasing the current pumping rate by 10% will result to a decrease in the amount of water gained by the river. Increasing the pumping rate by 20%, 30%, 40%, and 50% will reduce the amount of water gained by the river as shown in Figure 4.9. Increased pumping depletes the aquifer storage; hence, water would seep into the aquifer from the boundaries (Quitaneg, 2021).

In a study conducted by Gebere et al. (2021), it was established that an increase in pumping, and a decrease in recharge resulted in a decline in the amount of water flowing into the rivers and lakes. Indeed, the reduction in groundwater due to excessive pumping will result in low flows in the surface water and thus a lack of adequate water supply (Tian et al., 2015).

4.4.2 Scenario 2

In Scenario 2, the applied pumping schedule of 1040 m^3/day remained constant. However, climate change can affect the recharge rate and some aquifer boundaries. The Eastern side represents the water input into the groundwater aquifer, while the groundwater movement is westward. Therefore, any reduction in the groundwater level on this site will significantly affect the groundwater aquifer. Examining the impact of reducing the head imposed along the rivers and reducing recharge rate simultaneously reflect the effects of climate change. (Figures 4.9 and 4.10).

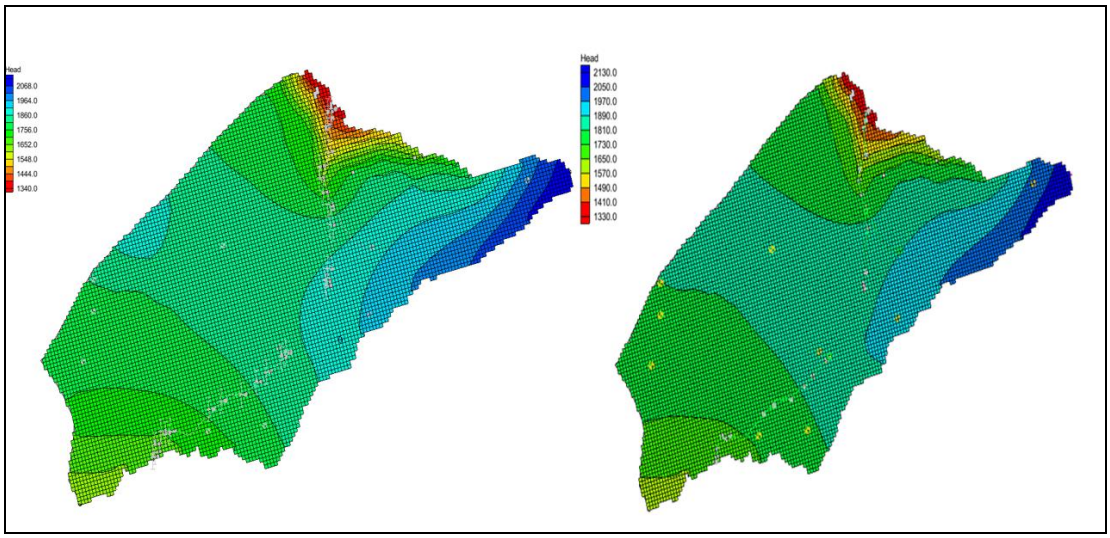

Figure 4.10: Comparison of the Computed Groundwater Table and Dry Areas with the Current Recharge Rate and 25% reduction of Recharge Rate, when the Specific Head is reduced by 5m

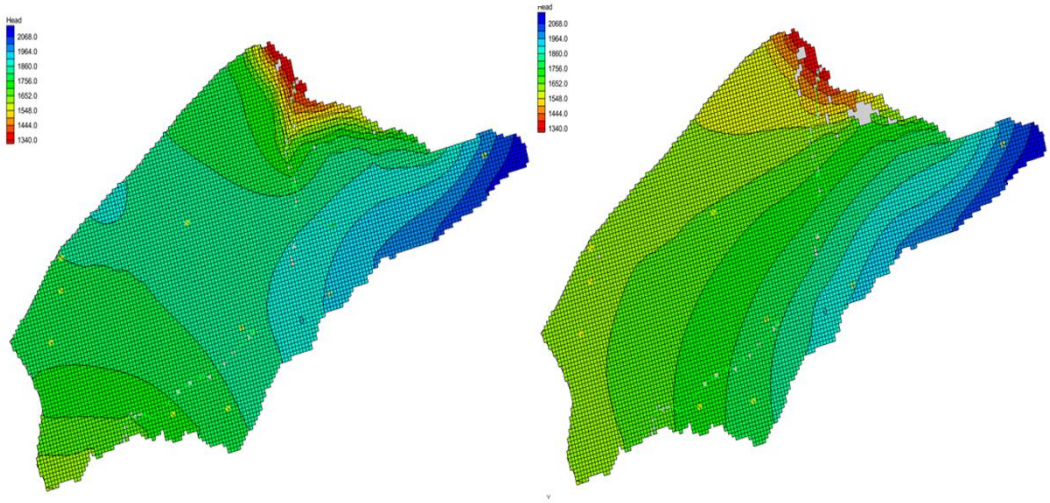

Figure 4.11: Comparison of the Computed Groundwater Table and Dry Areas with the Current Recharge Rate and 50 % reduction of Recharge Rate, when the Specific Head is Reduced by 5m

Comparing the increase in dry areas in both cases, it indicates the importance of specified head boundary. The dry areas increased due to the reduction of constant head (Sule & Ayenigba, 2017). Consequently, this influenced the pattern of groundwater equipotential lines, by pushing these equipotential lines towards the East side. Accordingly, the impact of decreasing the recharge rate in the study area was found to be greater than the impact of decreasing the constant head.

4.4.3 Scenario 3

The effect of reducing constant head by 5m and the recharge rate by 50%, and increasing the pumping rate by 50% at the same time was assessed. The results in this scenario are illustrated in Figure 4.11. There is a significant increase in the dry areas compared with scenario 2.

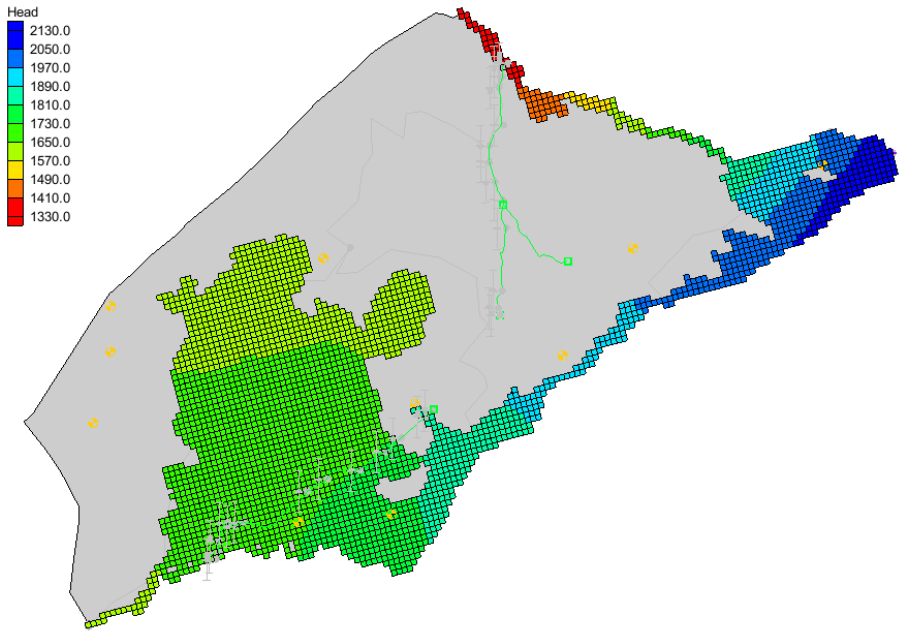

Figure 4.5: Computed groundwater table and dry areas with 50% increment on pumping rate and reduction of constant head and recharge by 5m and 50%, respectively

Table 4.8 shows the quantities of water lost and gained by the aquifer. The parameters studied in this regard include the storage, constant head, wells, drains and recharge.

Table 4.8: Water Budget Results for Scenario 3

Reducing constant head by 5m and Recharge by 50% and increasing pumping by 50%		
Parameter	**IN (m^3/day)**	**OUT (m^3/day)**
Storage	0	0
Constant Head	95947.02	55169.63
Wells	0	208.8
Drains	0	0
Recharge	0	40568.58
TOTAL IN=	95947.02	95947.01
IN-OUT=		0.02
PERCENT DISCREPANCY		-0.01

The overall effect of the reduction in the river level is the consequent reduction in water seepage from the river into the subsurface aquifer when the constant head is 5 m. The actual pumped water (1560 m^3/d) decreased to 208 m^3/day since most of the boreholes dried up. This scenario shows that climate change affects the water level in a river. However, the connection between the river and the aquifer remained effective despite the likely effects of climate change. Excessive pumping rates affect the interaction between surface water and groundwater. Depleting groundwater due to over-extraction has become one of the global challenges facing most countries (Konikow & Kendy, 2005).

In a study by Nagraj and Chetan (2017), a 3-D groundwater flow model, viz., Visual MODFLOW, was used with two conceptual layers. The model was simulated for seven years (2008–2014) under a transient case. The results from the modeling show that in the next ten years, the water table will decrease by more than 50m in the study area. The decrease in the water table was linked to climate change. From the scenarios analyzed, the authors suggested that reducing the pumping rate would help prevent future water scarcity.

Konikow (2013) examined groundwater depletion in the United States (1900–2008) in Reston, Virginia. The study reported groundwater depletion due to higher pumping than replenishment rates. Les et al. (2014) investigated the impacts of groundwater exploitation and climate change on wetland extension over 150 years. The study found that the degree of exploitation is an important parameter influencing the effects of groundwater pumping. Thus, climate change, alongside pressure from the increasing population, is likely to affect water availability in the Kericho aquifer significantly.

CHAPTER FIVE

CONCLUSION AND RECOMMENDATIONS

5.1 Conclusions

The following conclusions are drawned from this study:

1) It was observed that the aquifer thickness is high in the Northeastern (Kipkelion) and southwestern (Bureti) parts of the study area. Similarly, the highest value of spatial distribution of aquifer resistivity was observed in the southwestern part with an average of 976.9 Ω, and the lowest in the Northeastern part of the study area, which has an average of 376.75 Ω. Thus, it can be concluded that Kipkelion area has a great potential for groundwater, owing to the low values of aquifer resistivity and high conductive geomaterials. Moreover, the results show that Kaptaragon borehole is the most productive (SC = 125.84 M3/d/m, T = 728 m2/d) compared to boreholes in other locations within the study area. Hydraulic conductivity ranged from 0.279 m/d to 1.12 m/d, indicating that the area is dominated by coarse and fine sand. The highest value for hydraulic conductivity was recorded in Soin (1.12 m/d), while the lowest was recorded in Kipkelion (0.279 m/d).
2) The direction of groundwater movement is influenced by the level of groundwater. Moreover, discharge is typically highest in areas where the groundwater level is lowest. The heads distribution suggests that the groundwater flow in the area is from Northeast to West, indicating that pumping affects the direction of groundwater flow.
3) Scenario 1 results show that there was a minimal decrease in the level of groundwater near the drains and rivers. This can be attributed to the water transfer from the river to the aquifer. From the study findings, when there is no pumping from the groundwater aquifer, the river gains about 180,000 m^3/day of water. Accordingly, increasing the current pumping rate by 10% will result to a

decrease in the amount of water gained by the river. Scenario 2 shows that climate change will have an effect on the aquifers recharge rate. This will have an effect on the quantity of water in the aquifer in future. Scenario 3 shows that climate change affects the water level in a river. However, the connection between the river and the aquifer remained effective despite the likely effects of climate change. Furthermore, excessive pumping rates affect the interaction between surface water and groundwater. The volumetric budget for the three scenarios shows that the aquifer has sufficient water supply to be used by the population despite the effects of climate change and population growth.

5.2 Recommendations

The following are the Recommendations from this study

i. To ensure sustainability of future water supply in Kericho County and the neighboring counties, it is important that the policy makers and developers come up with appropriate measures to regulate the rates of groundwater pumping.
ii. Further studies should evaluate changes in the chemical property of water from the aquifer, due to the effects of pollution and climate change.
iii. In this study, Recharge was estimated to be 5% of the annual rainfall, therefore there is need to estimate recharge using physical techniques, water-budget methods, numerical modeling, and tracer methods.

REFERENCES

Abhishek, Gupta, P. K., & Yadav, B. K. (2022). Nutrient Loading Impact on Remediation of Hydrocarbon Polluted Groundwater Using Constructed Wetland. In *Wastewater Assessment, Treatment, Reuse and Development in India* (pp. 173-184). Cham: Springer International Publishing.

Abidin, M. Z., Saad, R., Ahmad, F., Wijeyesekera, D. C., & Baharuddin, M. T. (2012). Integral analysis of geoelectrical (resistivity) and geotechnical (SPT) data in slope stability assessment. *Academic Journal of Science*, *1*(2), 305-316.

Adeola Fashae, O., Abiola Ayorinde, H., Oludapo Olusola, A., & Oluseyi Obateru, R. (2019). Landuse and surface water quality in an emerging urban city. *Applied Water Science*, *9*, 1-12.

Adhikary, A., Konar, P., Chakraborty, T., & Pal, S. (2021, December). Assessment of Adsorptive Removal of Naphthalene Through Constructed Wetland Using Physical and Numerical Modeling. In *Indian Geotechnical Conference* (pp. 283-296). Singapore: Springer Nature Singapore.

Al Atawneh, D., Cartwright, N., & Bertone, E. (2021). Climate change and its impact on the projected values of groundwater recharge: A review. *Journal of Hydrology*, *601*, 126602.

Ameur, M., Aouiti, S., Hamzaoui-Azaza, F., Cheikha, L. B., & Gueddari, M. (2021). Vulnerability assessment, transport modeling and simulation of nitrate in groundwater using SI method and modflow-MT3DMS software: case of Sminja aquifer, Tunisia. *Environmental Earth Sciences*, *80*, 1-16.

Anderson, M. P., & Woessner, W. W. (1992). The role of the postaudit in model validation. *Advances in Water Resources*, *15*(3), 167-173.

Anderson, M., Woessner, W. & Hunt, R. (2015). Chapter 1. Introduction. 10.1016/B978-0-08-091638-5.00001-8.

Aquaveo (2011a) . *Groundwater Modelling System 7.1*. (Computer program)

Aquaveo website (2010) The New Groundwater Modeling System, 2010. Retrieved from http://www.aquaveo.com/gms.

Aquaveo, L. L. C. (2019). GMS User Manual 10.4. *Retrieved from GMS Wiki: https://www. xmswiki.com/wiki/GMS: GMS_User_Manual_10*, *4*.

Ashraf, M. A. M., Yusoh, R., Sazalil, M. A., & Abidin, M. H. Z. (2018, April). Aquifer characterization and groundwater potential evaluation in sedimentary rock formation. In *Journal of Physics: Conference Series* (Vol. 995, No. 1, p. 012106). IOP Publishing.

Barbieri, S. (2019). Adattamento del pacchetto connected linear network per la modellazione numerica di scambiatori geotermici in modflow-usg.

Barlow, P. M., & Leake, S. A. (2012). *Streamflow depletion by wells--Understanding and managing the effects of groundwater pumping on streamflow* (No. 1376, pp. i-84). US Geological Survey.

Barounis, N., & Karadima, K. (2011). Application of half Schlumberger configuration for detecting karstic cavities and voids for a wind farm site in Greece. *Journal of Earth Sciences and Geotechnical Engineering*, *1*(1), 101-116.

Beltrán, Guillermina Gómez, et al. (2013). Application of the Visual Modflow Model for the Evaluation of the Hydrodynamics of Underlying Aquifer to an Urban Solid Waste Sinter." *nternational Journal of Environmental Pollution 29*, 119-126.

Boel, S. (2008). *Hydrogeologische studie van de brownfield-site Vilvoorde-Machelen: grondwaterstromingen–transport [Hydrogeological study of the Vilvoorde-Machelen brownfield: groundwater fluxes and transport]* (Doctoral dissertation, MSc Thesis, Katholieke Universiteit Leuven, Belgium).

Botha, F. S. (2005). *A proposed method to implement a groundwater resource information project (GRIP) in rural communities, South Africa* (Doctoral dissertation, University of the Free State).

Boucher, M., Favreau, G., Vouillamoz, J. M., Nazoumou, Y., & Legchenko, A. (2009). Estimating specific yield and transmissivity with magnetic resonance sounding in an unconfined sandstone aquifer (Niger). *Hydrogeology Journal*, *17*(7), 1805.

Burazer, M., Žitko, V., Radaković, D., & Parezanović, M. (2010). Using geophysical methods to define the attitude and extension of water-bearing strata in the Miocene sediments of the Pannonian Basin. *Journal of Applied Geophysics*, *72*(4), 242-253.

Chalala, A., Chimbevo, L., Kahindo, J., Awadh, M., & Malala, J. (2017). Sea water intrusion and surface water salinity and its influence on irrigation water quality in Ramisi area, Kenya. *Journal of Agriculture and Ecology Research International*, *12*(1), 1-13.

Chen, J., Wu, H., Qian, H., & Li, X. (2018). Challenges and prospects of sustainable groundwater management in an agricultural plain along the Silk Road Economic Belt, north-west China. *International journal of water resources development*, *34*(3), 354-368.

Chen, Z., Huang, J., Zhan, H., Wang, J., Dou, Z., Zhang, C., ... & Fu, Y. (2022). Optimization schemes for deep foundation pit dewatering under complicated

hydrogeological conditions using MODFLOW-USG. *Engineering Geology*, *303*, 106653.

Cirpka, O. A., & Valocchi, A. J. (2016). Debates—Stochastic subsurface hydrology from theory to practice: Does stochastic subsurface hydrology help solving practical problems of contaminant hydrogeology?. *Water Resources Research*, *52*(12), 9218-9227.

Cooper Jr, H. H., & Jacob, C. E. (1946). A generalized graphical method for evaluating formation constants and summarizing well-field history. *Eos, Transactions American Geophysical Union*, *27*(4), 526-534.

Cuthbert, M. O., Taylor, R. G., Favreau, G., Todd, M. C., Shamsudduha, M., Villholth, K. G. ... & Lawson, F. M. (2019). Observed controls on resilience of groundwater to climate variability in sub-Saharan Africa. *Nature*, *572*(7768), 230-234.

de Almeida, A., Maciel, D. F., Sousa, K. F., Nascimento, C. T. C., & Koide, S. (2021). Vertical electrical sounding (VES) for estimation of hydraulic parameters in the porous aquifer. *Water*, *13*(2), 170

Debbarma, S., & Dutta, A. (2016). Utilizing electric vehicles for LFC in restructured power systems using fractional order controller. *IEEE transactions on smart grid*, *8*(6), 2554-2564.

Domenico, P. A., & Schwartz, F. W. (1997). *Physical and chemical hydrogeology*.(2nd ed). John wiley & sons.

Dong, Y., Safferman, S. I., & Pouyan Nejadhashemi, A. (2019). Computational modeling of wastewater land application treatment systems to determine strategies to improve carbon and nitrogen removal. *Journal of Environmental Science and Health, Part A*, *54*(7), 657-667.

Driscoll, F. G. (1986). Groundwater and wells. (2nd ed). *St. Paul*.

Egbai, J. C., Aigbogun, C. O., Adaikpoh, E. O., & Pius, E. (2013). Resistivity model: a tool for coastal aquifer assessment in Okwuagbe community of Delta State, Nigeria. *Technical Journal of Engineering and Applied Sciences, 3*(19), 2357-2364.

El-Rawy, M., Makhloof, A. A., Hashem, M. D., & Eltarabily, M. G. (2021). Groundwater management of quaternary aquifer of the Nile Valley under different recharge and discharge scenarios: A case study Assiut governorate, Egypt. *Ain Shams Engineering Journal*, *12*(3), 2563-2574.

Ezzeldin, M., El-Alfy, K., Abdel-Gawad, H., & Abd-Elmaboud, M. (2018). Comparison between structured and unstructured MODFLOW for simulating groundwater flow in three-dimensional multilayer quaternary aquifer of East Nile Delta, Egypt. *Hydrol Curr Res*, *9*, 297.

Ferrer, N., Folch, A., Lane, M., Olago, D., Odida, J., & Custodio, E. (2019). Groundwater hydrodynamics of an Eastern Africa coastal aquifer, including La Niña 2016–17 drought. *Science of the total environment*, *661*, 575-597.

Foster, L. M., & M. Maxwell, R. (2019). Sensitivity analysis of hydraulic conductivity and Manning's n parameters lead to new method to scale effective hydraulic conductivity across model resolutions. *Hydrological Processes*, *33*(3), 332-349.

Freeze, R. A., & Cherry, J. A. (1979). Groundwater prentice-hall. *Englewood Cliffs, NJ*, *176*, 161-177.

Gallardo, A. H. (2016). Groundwater Exploration for Rural Water Supply in an Arid Region of Southern Argentina. *Geosciences*, *6*(2), 28.

Gebere, A., Kawo, N. S., Karuppannan, S., Hordofa, A. T., & Paron, P. (2021). Numerical modeling of groundwater flow system in the Modjo River catchment, Central Ethiopia. *Modeling Earth Systems and Environment*, *7*(4), 2501-2515.

Goulburn-Murray Water, (2015). Ovens Basin, Retrieved from http://www. g-mwater.com.au/water-resources/catchments/ovensbasin

Hamisi, R., Renman, A., Renman, G., Wörman, A., & Thunvik, R. (2022). Long-term phosphorus sorption and leaching in sand filters for onsite treatment systems. *Science of the Total Environment*, *833*, 155254.

Harbaugh, A. W. (2005). *MODFLOW-2005, the US Geological Survey modular ground-water model: the ground-water flow process* (Vol. 6). Reston, VA, USA: US Department of the Interior, US Geological Survey.

Hariharan, V., & Shankar, M. U. (2017, November). A review of visual MODFLOW applications in groundwater modelling. In *IOP Conference Series: Materials Science and Engineering* (Vol. 263, No. 3, p. 032025). IOP Publishing.

Hill, M. C., Barlebo, H. C., Rosbjerg, D., & Jensen, K. H. (1998). Concentration data and dimensionality in groundwater models: Evaluation using inverse modelling. *Hydrology Research*, *29*(3), 149-178.

Holland, R. A., Scott, K. A., Flörke, M., Brown, G., Ewers, R. M., Farmer, E., ... & Eigenbrod, F. (2015). Global impacts of energy demand on the freshwater resources of nations. *Proceedings of the National Academy of Sciences*, *112*(48), E6707-E6716.

Huang, C. C., & Yeh, H. F. (2019). Hydrogeological Parameter Determination in the Southern Catchments of Taiwan by Flow Recession Method. *Water*, *11*(1), 7.

Jafari, T., Kiem, A. S., Javadi, S., Nakamura, T., & Nishida, K. (2021). Fully integrated numerical simulation of surface water-groundwater interactions using SWAT-MODFLOW with an improved calibration tool. *Journal of Hydrology: Regional Studies*, *35*, 100822.

JafJICA, (2013). National water master plan 2030. Draft 1. JICA. Nairobi, Kenya

Joint Monitoring and Program (2015): Annual Report WHO/UNICEF, Joint Monitoring Programme for Water Supply and Sanitation.

Karamouz, M., Ahmadi, A., & Akhbari, M. (2020). *Groundwater hydrology: Engineering, planning, and management*. CRC press.

Kasenow, M. (2006). *Aquifer test data: analysis and evaluation*. Water Resources Publication.

Kericho County Government, (20122). Integrated Development Plan 2018/2022, doi: 10.1177/1066480798061020

Knüppe, K. (2011). The challenges facing sustainable and adaptive groundwater management in South Africa. *Water Sa*, *37*(1).

Konikow, L. F. (2013). *Groundwater depletion in the United States (1900− 2008)* (No. 2013-5079). US Geological Survey.

Konikow, L. F., & Kendy, E. (2005). Groundwater depletion: A global problem. *Hydrogeology journal*, *13*, 317-320.

Krásný, J. (1993). Classification of transmissivity magnitude and variation. *Groundwater*, *31*(2), 230-236.

Kumar, C. P. (2012). Groundwater modelling software–capabilities and limitations. *IOSR Journal of Environmental Science, Toxicology and Food Technology*, *1*(2), 46-57.

Kumar, G. P., & Kumar, P. A. (2014). Development of groundwater flow model using visual MODFLOW. *Internat. Jour. Advd. Res*, *26*, 649-656.

Kuria, Z. (2013). Groundwater distribution and aquifer characteristics in Kenya. In *Developments in earth surface processes* (Vol. 16, pp. 83-107). Elsevier.

Kurniawan, A. (2009). Basic IP@ Win Tutorial. *Hydrogeology World*.

Lee, H. (2018). MODFLOW with Flopy (1): Intro & Installation.

Les Landes, A. A., Aquilina, L., De Ridder, J., Longuevergne, L., Pagé, C., & Goderniaux, P. (2014). Investigating the respective impacts of groundwater exploitation and climate change on wetland extension over 150 years. *Journal of Hydrology*, *509*, 367-378.

Li, X., Li, D., Xu, Y., & Feng, X. (2020). A DFN based 3D numerical approach for modeling coupled groundwater flow and solute transport in fractured rock mass. *International Journal of Heat and Mass Transfer*, *149*, 119179.

Li, X., Li, D., Xu, Y., & Feng, X. (2020). A DFN based 3D numerical approach for modeling coupled groundwater flow and solute transport in fractured rock mass. *International Journal of Heat and Mass Transfer*, *149*, 119179.

Liu, W., Park, S., Bailey, R. T., Molina-Navarro, E., Andersen, H. E., Thodsen, H., ... & Trolle, D. (2020). Quantifying the streamflow response to groundwater abstractions for irrigation or drinking water at catchment scale using SWAT and SWAT–MODFLOW. *Environmental Sciences Europe*, *32*, 1-25.

Long, D., Yang, W., Scanlon, B. R., Zhao, J., Liu, D., Burek, P., ... & Wada, Y. (2020). South-to-North Water Diversion stabilizing Beijing's groundwater levels. *Nature Communications*, *11*(1), 3665.

Matos, C. R., Carneiro, J. F., & Silva, P. P. (2019). Overview of large-scale underground energy storage technologies for integration of renewable energies and criteria for reservoir identification. *Journal of Energy Storage*, *21*, 241-258.

Maxwell, R. M., & Condon, L. E. (2016). Connections between groundwater flow and transpiration partitioning. *Science*, *353*(6297), 377-380.

McDonald, M. G., & Harbaugh, A. W. (1988). *A modular three-dimensional finite-difference ground-water flow model*. US Geological Survey.

Melaku, N. D., & Wang, J. (2019). A modified SWAT module for estimating groundwater table at Lethbridge and Barons, Alberta, Canada. *Journal of Hydrology*, *575*, 420-431.

Mwiathi, N. F., Gao, X., Li, C., & Rashid, A. (2022). The occurrence of geogenic fluoride in shallow aquifers of Kenya Rift Valley and its implications in groundwater management. *Ecotoxicology and Environmental Safety*, *229*, 113046.

Nagraj, S. P. (2017). Groundwater Modeling of Hiranyakeshi Watershed of Ghataprabha Sub-basin. *Journal geological society of India*, *90*, 357-361.

Namitha, M. R., JS, D. K., & Sreelekshmi, H. (2019). Ground water flow modelling using visual modflow. *Journal of Pharmacognosy and Phytochemistry*, *8*(1), 2710-2714.

Nejad, H. T. (2009). Geoelectric investigation of the aquifer characteristics and groundwater potential in Behbahan Azad University Farm, Khuzestan Province, Iran. *Journal of Applied Sciences*, *9*(20), 3691-3698.

Omar, P. J., Gaur, S., Dwivedi, S. B., & Dikshit, P. K. S. (2020). A modular three-dimensional scenario-based numerical modelling of groundwater flow. *Water Resources Management*, *34*(6), 1913-1932.

Pandey, V. P., & Kazama, F. (2011). Hydrogeologic Characteristics of Groundwater Aquifers in Kathmandu Valley, Nepal. *Environmental Earth Sciences*, *62*(8), 1723-1732. http://dx.doi.org/10.1007/s12665-010-0667-3.

Park, B. H., Lee, B. H., & Lee, K. K. (2018). Experimental investigation of the thermal dispersion coefficient under forced groundwater flow for designing an optimal groundwater heat pump (GWHP) system. *Journal of hydrology*, *562*, 385-396.

Pavelic, P., Giordano, M., Keraita, B. N., Ramesh, V., & Rao, T. (2012). *Groundwater availability and use in Sub-Saharan Africa: a review of 15 countries*. International Water Management Institute.

Perrone, D., & Jasechko, S. (2017). Dry groundwater wells in the western United States. *Environmental Research Letters*, *12*(10), 104002.

Pervez, M. S., & Henebry, G. M. (2015). Assessing the impacts of climate and land use and land cover change on the freshwater availability in the Brahmaputra River basin. *Journal of Hydrology: Regional Studies*, *3*, 285-311.

Peterson, T. J., & Fulton, S. (2019). Joint Estimation of Gross Recharge, Groundwater Usage, and Hydraulic Properties within HydroSight. *Groundwater*, *57*(6), 860-876.

Quitaneg, L. C. (2021, December). GMS-MODFLOW application in the investigation of groundwater potential in Concepcion, Tarlac, Philippines. In *IOP Conference Series: Earth and Environmental Science* (Vol. 958, No. 1, p. 012005). IOP Publishing.

Rossetto, R., De Filippis, G., Borsi, I., Foglia, L., Cannata, M., Criollo, R., & Vázquez-Suñé, E. (2018). Integrating free and open source tools and distributed modelling codes in GIS environment for data-based groundwater management. *Environmental Modelling & Software*, *107*, 210-230.

Sahoo, S., & Jha, M. K. (2017). Numerical groundwater-flow modeling to evaluate potential effects of pumping and recharge: implications for sustainable groundwater management in the Mahanadi delta region, India. *Hydrogeology journal*, *25*(8), 2489-2511.

Shaban, A., Khawlie, M., & Abdallah, C. (2006). Use of remote sensing and GIS to determine recharge potential zones: the case of Occidental Lebanon. *Hydrogeology Journal*, *14*, 433-443.

Sule, B. F., & Ayenigba, S. E. (2017). Application of GMS-MODFLOW to investigate groundwater development potential in River Meme catchment, Kogi State, Nigeria. *International Journal of Sciences*, *6*(09), 39-51.

Szymkiewicz, A., Gumuła-Kawęcka, A., Šimůnek, J., Leterme, B., Beegum, S., Jaworska-Szulc, B., ... & Jacques, D. (2018). Simulations of freshwater lens recharge and salt/freshwater interfaces using the HYDRUS and SWI2 packages for MODFLOW. *Journal of Hydrology and Hydromechanics*, *66*(2), 246-256.

Tamma Rao, G., Gurunadha Rao, V. V. S., Surinaidu, L., Mahesh, J., & Padalu, G. (2013). Application of numerical modeling for groundwater flow and contaminant transport analysis in the basaltic terrain, Bagalkot, India. *Arabian Journal of Geosciences*, *6*, 1819-18

Tian, Y., Zheng, Y., Wu, B., Wu, X., Liu, J., & Zheng, C. (2015). Modeling surface water-groundwater interaction in arid and semi-arid regions with intensive agriculture. *Environmental Modelling & Software*, *63*, 170-184.

Touchant, K., Bronders, J., Patyn, J., Seuntjens, P., Lookman, R., & Joris, I. (2007). *Brownfield problematiek Vilvoorde-Machelen: risicomanagement regionale grondwaterverontreiniging [The problematic Vilvoorde-Machelen brownfield: risk management and regional groundwater pollution]*. Report 2007/IMS/43, VITO, Mol, Belgium.33.

Vsevolozhsky, V.A., (2009). Groundwater in Sedimentary, Metamorphic and Volcanic Rocks. *Hydrological Cycle* , 4 118 – 127, 2003.

Wang, Y., Ma, R., Wang (2018). Groundwater sustainability in fast-developing China. *Hydrogeol J*, 26, 1295–1300

Wu, J., & Sun, Z. (2016). Evaluation of Shallow Groundwater Contamination and Associated Human Health Risk in an Alluvial Plain Impacted by Agricultural and Industrial activities, mid-west China. *Exposure and Health*, *8*(3), 311–329

Yifru, B. A., Chung, I. M., Kim, M. G., & Chang, S. W. (2020). Assessment of groundwater recharge in agro-urban watersheds using integrated SWAT-MODFLOW model. *Sustainability*, *12*(16), 6593.

Yihdego, Y., & Webb, J. A. (2018). Comparison of evaporation rate on open water bodies: energy balance estimate versus measured pan. *Journal of Water and Climate Change*, *9*(1), 101-111.

Zhai, X., Shen, S., Wu, J., & Han, D. (2014). Drainage Evaluation of Limestone Aquifer Based on Visual Modflow.

Zhang, H., Yang, R., Guo, S., & Li, Q. (2020). Modeling fertilization impacts on nitrate leaching and groundwater contamination with HYDRUS-1D and MT3DMS. *Paddy and Water Environment*, *18*, 481-498.

Zong, Y., Valocchi, A. J., & Lin, Y. F. F. (2021). Coupling a borehole thermal model and MT3DMS to simulate dynamic ground source heat pump efficiency. *Groundwater*.

APPENDICES

Appendix I: Variation of Aquifer Resistivity and Thickness

		Layer 1		layer 2		Layer 3		Layer 4		Layer 5		Layer 6	
ves station	***Borehole Name***	***Resistivity***	***Thickness(m)***	***Resistivity***	***Thickness(m)***	***Resistivity***	***Thickness(m)***	***Resistivity***	***Thickness(m)***	***Resistivity***	***Thickness(m)***	***Resistivity***	***Thickness(m)***
ves 1	Motero	507.3	1.3	236.9	3.6	390.9	10	21.8	47	81.1	_	_	_
ves 2	Tingatela	293.02	1	20.08	6.2	39.239	24.1	13.699	56	139.13	_	_	_
ves 3	Lelaitich idp camp	13.7	3.8	221.6	18	99.6	44.1	589.8	_	_	_	_	_
ves 4	Sunshine	82	1	576	1.9	91	30	902	100	_	_	_	_
ves 5	Aic Tumaini	135.72	4.3	73.924	26	17.166	_	_	_	_	_	_	_
ves 6	Atc Kipsitet	41.8	1	33.8	10	550.8	34	10.1	_	_	_	_	_
ves 7	Asenewet	463.9	0.8	31.9	8	209.5	60.3	38.6	135	148.5	_	_	_
ves 8	Kaptaragon	134	1.3	23.3	9.5	104.9	43	335.6	197	41.9	_	_	_
ves 9	Lemotit Atletic camp	1481.3	1.2	13.993	17	33.997	44	354.46	_	_	_	_	_
ves 10	Masasita hills area	246.8	0.6	19.247	7.7	41.711	14	17.102	120	_	_	_	_
ves 11	Emdit Primary	2034.9	0.7	98.419	2.7	189.52	90	581.83	_	_	_	_	_
ves 12	Sosit	433.2	4	8.1	68	85	_	_	_	_	_	_	_
ves 13	Kusumek	323.7	2.5	26.3	9.6	153.4	15.1	2267.1	_	_	_	_	_
ves 14	Ewat	52.4	0.6	25.8	5	219.9	27	90.9	57	1579	_	_	_
ves 15	Seretet	110.3	0.6	323.5	7	157.4	43	170.6	108	154.9	148	224.2	_
ves 16	Cheptororiet	729.71	1.6	439.42	16	51.136	68.2	103.46	_	_	_	_	_
ves 17	Soget	234.5	2	14.3	10	25.6	18	10	74	259.7	_	_	_
ves 18	Sototwet	72.6	1.1	196.7	9.1	49.3	53	477.5	_	_	_	_	_
ves 19	Ngendalel	329.5	1.1	120	3.5	620.5	16.7	495.9	50	1342.01	114.3	981.3	_
ves 20	Kapsomboch	395.9	13.1	72	63.5	444.9	120	507.6	_	_	_	_	_
ves 21	Butiik	416	1.28	54	19.57	251	21.46	2000	_	_	_	_	_
ves 22	Kapsewa	1126.7	2.1	213	17.2	131.3	37.7	186.1	113.7	1126.7	_	_	_
ves 23	Tulwet	486.8	2.2	248.1	7.2	14.7	120.8	139.9	_	_	_	_	_

ves 24	Kipreng we	118 3.4	1.1	17.8 13	13	304. 96	57	32.4 777	232	136. 26	_	_	_
ves 25	Kamolok	50.7 02	2	68.7	9	12	33.7	77.5	101.6	37.9	_	_	_
ves 26	Koiwalel ach	904. 9	2	283. 3	7.2	516. 6	18	300. 4	36	687. 7	_	_	_
ves 27	Lelechw et	270 4	0.9	7.1	4	3.1	140	9.3	_	_	_	_	_
ves 28	Kamaget	81.8	4.8	51.4	12.2	16	40	373. 1	_	_	_	_	_
ves 29	Kaptugu mo	115. 2	2.1	91.9	17.2	30.7	37.7	52.9	113.7	29.9	_	_	_
ves 30	Kabloin	223	2	80.8	7.2	110 9.5	85.2	80	264	489. 5	_	_	_
ves 31	Kapchel uch	372. 3	1.8	126. 6	22.7	34.6	87.5	165. 2	87.5	165. 2	_	_	_
ves 32	Tingoro	144 1.3	2	51.8	16.3	117	63	55	192	124	_	_	_
ves 33	Ketisyek	73.6	0.7	265. 9	2.5	67.8	10	12.5	28	454. 7	_	_	_
ves 34	Katet	556. 1	1	12.4	18.2	58.7	77	22.2	118	366. 9	_	_	_
ves 35	Kapsoge ruk	165. 7	0.4	49.2	1.2	87.8	5	16.2	26.1	701. 5	_	_	_
ves 36	Kapkond or	207. 3	1.4	48	6	11	13	122. 5	70	23.7	_	_	_
ves 37	Kabatet	619 22	4.7	563	14.6	103. 8	146.1	269. 4	_	_	_	_	_
ves 38	Kibugat	99.7	5.6	15.9	16.5	388. 2	44.5	552 9.3	_	_	_	_	_
ves 39	Mosore	460 0.1	1	171 4.2	6	695. 6	41	98.4	_	_	_	_	_
ves 40	Kondam et	81.5	1.7	252. 3	4.5	54.1	71.6	162. 9	_	_	_	_	_
ves 41	Kisabei	86.7	2	341. 8	5	71.9	83	193. 7	125	587. 1	_	_	_
ves 42	Sosiot Girls	915. 1	0.8	202. 7	3.5	474. 2	88	137. 7	_	_	_	_	_
ves 43	Ngororg a	393. 12	0.8	134. 12	7	27.7 23	26	75.9 14	71	151 6.2	_	_	_
ves 44	Kapkebu ru	419. 27	4.8	216. 1	26	430. 82	72.1	60.1 94	_	_	_	_	_
ves 45	Cheribo	891. 2	0.4	406 8.4	1.5	256. 7	21.6	94	157.2	524. 3	_	_	_
ves 46	Kipsegi	298. 66	0.5	17.3 87	2	216. 76	8.5	70.0 82	51	18.5 84	223	33.7 53	_
ves 47	Koituk	195. 34	1.1	62.3 31	12	12.4 67	49	148. 4	_	_	_	_	_
ves 48	Chelilis	104. 9	0.7	333. 2	5.6	25.9	47.9	281. 7	160.7	91.7	244	118. 8	_
ves 49	Chebirir	9.9	6.5	70.8	38.6	41.9	71	509. 4	_	_	_	_	_
ves 50	Arokyet	124. 4	0.9	39.2	2	99.1	4.1	42.1	10.6	117. 3	80.6	42.1	_

Appendix II: Site Photos

Appendix III: Borehole Information

S/No	Borehole Name	Yield(M^3/hr.)	Actual Borehole Depth(m)	Static Water Level(m)	Borehole radius(m)	Casing radius(m)
1	TAPSABEI KORIR	4.32	110	22.2	0.075	0.11
2	RONALD CHERUIYOT	1.8	120	11.9	0.075	0.11
3	EVERGREEN TEA FACTORY LTD	2	200	24.6	0.075	0.11
4	CHEPKEMEL PRIMARY SCHOOL	5.54	151	36	0.075	0.11
5	CHEPNGOBOB PRI	7	120	49.83	0.075	0.11
6	CHEBWAGAN	1.2	200	131.47	0.075	0.11
7	CHERES	10	150	60	0.075	0.11
8	KABOKYEK	4.1	160	32.26	0.075	0.11
9	KAMUINGI	2.5	102	49.73	0.075	0.11
10	KAPCHELUCH	6	170	82.17	0.075	0.11
11	KAPKATET HOSPITAL	4.3	160	77.33	0.075	0.11
12	KAPKISIARA	4	180	34.27	0.075	0.11
13	KAPTARAGON	9.7	230	164.27	0.075	0.11
14	KATET	7	125	49.73	0.075	0.11
15	KIBOET	1.7	190	151.54	0.075	0.11
16	KIBUGAT	3.1	130	43.46	0.075	0.11
17	KIPSITET	6	60	50.4	0.075	0.11
18	LELDET	5.3	120	10	0.075	0.11
19	LEMOTIT	0.7	45	21.33	0.075	0.11
20	LONDIANI	4	150	24.17	0.075	0.11
21	MOTERO	6	205	98.04	0.075	0.11
22	SERETET/CHEPTORORIET	1.9	205	82.02	0.075	0.11
23	SIGOWET HOSPITAL	3.5	75	21.33	0.075	0.11
24	SOLIAT	6	205	98.04	0.075	0.11

Appendix IV: Location of the VES stations

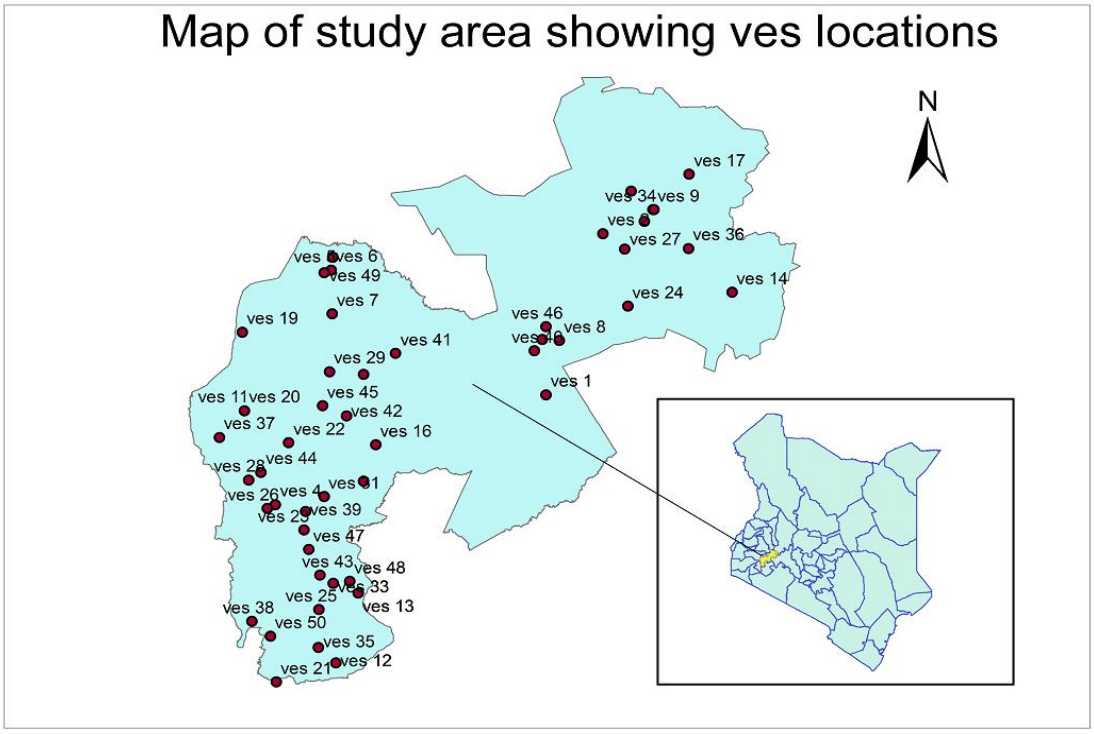

Appendix V: Kericho County Administration Areas

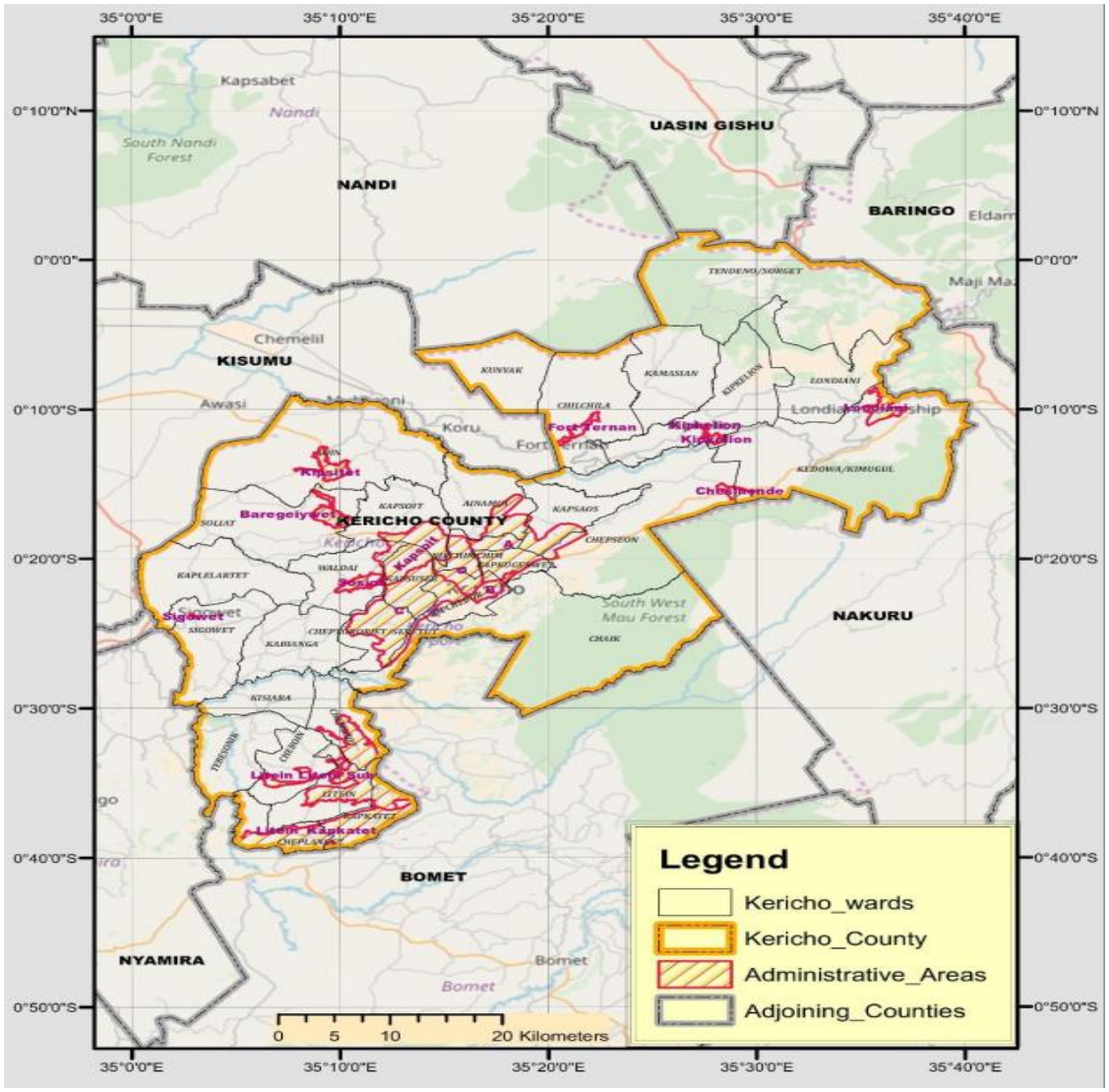

Appendix 6: Summary of Ves Analysis

ves station	Borehole Name	Aquifer Resistivity	Aquifer Thickness(m)	Longitudinal conductance	Hydraulic Conductivity	Transmissivity	Eastings	Southings	Groundwater Potential
ves 1	Motero	413	57	0.1381	1.4031	79.9778	766699	9963342	Intermediate
ves 2	Tingatela	53	80	1.5131	9.5292	763.2865	773622	9983746	High
ves 3	Lelaitich idp camp	689	44	0.0640	0.8694	38.3411	740622	9980746	Intermediate
ves 4	Sunshine	993	130	0.1309	0.6186	80.4149	733630	9949456	Intermediate
ves 5	Aic Tumaini	91	26	0.2854	5.7436	149.3336	740423	9979116	High
ves 6	Atc Kipsitet	561	34	0.0606	1.0539	35.8322	740451	9979147	Intermediate
ves 7	Asenewet	248	195	0.7872	2.2556	440.5140	740545	9973587	High
ves 8	Kaptaragon	441	240	0.5448	1.3203	316.8811	768312	9970197	High
ves 9	Lemotit Atletic camp	388	44	0.1133	1.4846	65.3240	779758	9986775	Intermediate
ves 10	Masaita hills area	59	134	2.2784	8.6381	1157.5083	778728	9985307	Very high
ves 11	Emdit Primary	771	90	0.1167	0.7829	70.4636	729847	9961334	Intermediate
ves 12	Sosit	91	26	0.2857	5.7483	149.4560	740984	9929440	High
ves 13	Kusumek	2421	15	0.0062	0.2694	4.0682	743723	9938239	Low
ves 14	Ewat	311	84	0.2703	1.8280	153.5520	789418	9976298	High
ves 15	Seretet	263	256	0.9738	2.1369	547.0460	744412	9952428	High
ves 16	Cheptororiet	155	68	0.4411	3.5066	239.1507	745880	9956998	High
ves 17	Soget	36	92	2.5843	13.7974	1269.3630	784201	9991265	Very high
ves 18	Sototwet	527	53	0.1006	1.1174	59.2216	744388	9965912	Intermediate
ves 19	Ngendalel	2334	164	0.0704	0.2787	45.7975	729583	9971285	Intermediate
ves 20	Kapsomboch	953	120	0.1260	0.6431	77.1692	729847	9961334	Intermediate
ves 21	Butiik	2251	21	0.0095	0.2883	6.1869	733735	9926998	Low
ves 22	Kapsewa	317	151	0.4770	1.7925	271.3870	735249	9957264	High
ves 23	Tulwet	155	121	0.7814	3.5065	423.5881	737153	9946223	High
ves 24	Kiprengwe	337	289	0.8565	1.6930	489.2830	776692	9974564	High
ves 25	Kamolok	90	135	1.5117	5.8387	789.9795	738919	9936149	High

ves 26	Koiwalelach	817	54	0.0661	0.7420	40.0703	732672	9948978	Intermediate
ves 27	Lelechwet	12	140	11.2903	36.9029	5166.4068	776329	9981806	Very high
ves 28	Kamaget	389	40	0.1028	1.4823	59.2939	730379	9952564	Intermediate
ves 29	Kaptugumo	84	151	1.8110	6.2222	942.0443	740219	9966268	High
ves 30	Kabloin	1190	349	0.2936	0.5227	182.5236	766250	9970345	High
ves 31	Kapcheluch	200	175	0.8759	2.7604	483.0707	739594	9950434	High
ves 32	Tingoro	172	255	1.4826	3.1745	809.4859	777079	9989145	High
ves 33	Ketisyek	80	38	0.4732	6.4604	245.4963	740692	9939499	High
ves 34	Katet	81	195	2.4104	6.4157	1251.0657	779881	9986769	Very high
ves 35	Kapsogeruk	104	31	0.2990	5.0756	157.8513	738881	9931365	High
ves 36	Kapkondor	134	83	0.6217	4.0209	333.7356	784114	9981861	High
ves 37	Kabatet	373	146	0.3915	1.5412	225.1661	726785	9957965	High
ves 38	Kibugat	5918	45	0.0075	0.1170	5.2075	730774	9934688	Low
ves 39	Mosore	794	41	0.0516	0.7621	31.2451	737313	9948566	Intermediate
ves 40	Kondamet	217	72	0.3300	2.5557	182.9913	765247	9968900	High
ves 41	Kisabei	266	208	0.7831	2.1166	440.2585	748311	9968581	High
ves 42	Sosiot Girls	612	88	0.1438	0.9717	85.5107	742317	99600659	Intermediate
ves 43	Ngororga	104	97	0.9360	5.0922	493.9422	739042	9940494	High
ves 44	Kapkeburu	491	72	0.1468	1.1932	86.0279	731892	9953546	Intermediate
ves 45	Cheribo	351	179	0.5098	1.6332	292.0197	739370	9961957	High
ves 46	Kipsegi	89	274	3.0902	5.8899	1613.8435	766713	9971970	Very high
ves 47	Koituk	161	49	0.3046	3.3789	165.5673	737709	9943761	High
ves 48	Chelilis	373	405	1.0838	1.5404	623.4031	742687	9939710	High
ves 49	Chebirir	551	71	0.1288	1.0710	76.0408	739607	9978818	Intermediate
ves 50	Arokyet	159	91	0.5721	3.4079	310.8027	732999	9932775	High
		573	**120**	**0.8547**	**3.6239**	**440.5239**			